

UC-NRLF



C 3 138 831

1

FSL

PHYSICAL
SCIENCES
LIBRARY

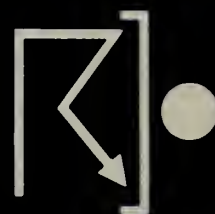
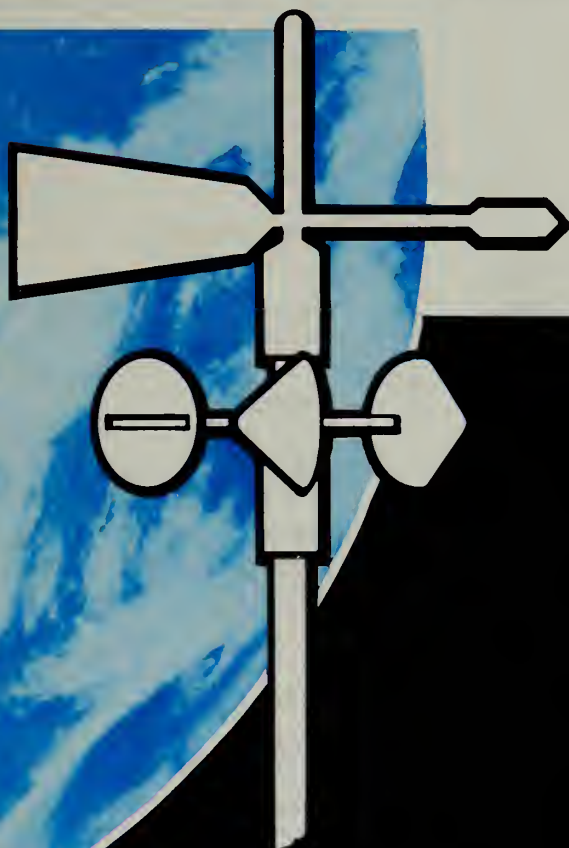
**POLARIZATION OF SKYLIGHT
AT AN ALTITUDE OF 3461 METERS
ON MAUNA LOA, HAWAII**

UNIVERSITY OF CALIFORNIA
DAVIS

DEC 3 1974

SER. REC. LIBRARY

by K.L. Coulson, R.L. Walraven, L.B. Soohoo



Contributions in Atmospheric Science No. 9
UNIVERSITY OF CALIFORNIA - DAVIS

NOV 6 1975

Department of Agricultural Engineering
University of California
Davis, California


Polarization of Skylight
at an Altitude of 3416m (11200 ft)
on Mauna Loa, Hawaii

by

Kinsell L. Coulson
Robert L. Walraven
Leon B. Soohoo

Final Report
Grant No. N-22-161-72(N)
Air Resources Laboratories
National Oceanic and Atmospheric Administration
Silver Spring, Maryland
in conjunction with
Grant No. NGL 05-003-404
National Aeronautics and Space Administration
Washington, D.C.

March, 1974



Digitized by the Internet Archive
in 2012 with funding from
University of California, Davis Libraries

<http://www.archive.org/details/polarizationofsk09coul>

Abstract

In order to take advantage of the sensitivity of skylight polarization to dust, haze, and other particulate matter for characterizing atmospheric turbidity, a series of measurements of skylight polarization was made at the Mauna Loa Observatory during February and March of 1973. The polarizing radiometer used for the measurements provided data in eight narrow bands in the ultraviolet, visible and near infrared spectral regions. Results obtained show that the skylight polarization field at Mauna Loa is much more variable than had been anticipated. While certain aerosol effects show up in the data, they are combined with equally large variations which appear to be unrelated to atmospheric turbidity. A preliminary interpretation indicates that these non-aerosol effects are probably due to variable reflection properties of clouds and sea surface surrounding the island. If this interpretation is correct, then future measurements for characterizing atmospheric turbidity at Mauna Loa should be made during selected periods of cloudless conditions in the area. In this case the dark lava of the mountain and low albedo of the surrounding sea surface should minimize reflection effects and permit valid and consistent conclusions on atmospheric turbidity at Mauna Loa on a long-term basis.

Table of Contents

	Page
Abstract	i
Table of Contents	ii
List of Tables	iii
List of Figures	iv
I Introduction	1
II Instrumentation and Operational Procedures	2
III Results of Measurements	6
A. Typical Polarization Distribution	6
B. Spectral Distribution of the Polarization Maximum	11
C. Positions of the Neutral Points	16
IV Comparison with Theory	24
V Parameterization of the Polarization Field	28
VI Discussion	38
VII Conclusions	47
VIII References	48
IX Acknowledgment	49

List of Tables

	Page
Table 1. Normal optical thickness at the Mauna Loa Observatory for a Rayleigh atmosphere at wavelength of peak transmissions of the optical filters used in these measurements.	24
Table 2. Types of clouds and total sky cover from the Hilo weather observation station and the large scale cloud indications from satellite photographs of the Pacific area.	42
Table 3. Approximate optical pathlength τ and fractional transmission T at wavelengths of 0.32 and 0.90 μ m for the intensity component I_s due to sea surface reflection for locations at the sea surface itself, at the observation site, and at the top of the atmosphere for two different zenith angles θ_o of the sun.	46

List of Figures

Figure		Page
1.	Schematic diagram of one of the two channels of the photon-counting polarizing radiometer.	4
2.	Typical data on the degree of linear polarization of skylight, as measured by the photon-counting polarizing radiometer.	7
3.	Degree of polarization of skylight in the sun's vertical as observed in two wavelengths during four different scans of the sky at Mauna Loa on March 25, 1973. ($\lambda = 0.32$ and $0.60\mu\text{m}$).	9
4.	Degree of polarization of skylight in the sun's vertical as observed in two wavelengths during three different scans of the sky at Mauna Loa on March 25, 1973. ($\lambda = 0.50$ and $0.90\mu\text{m}$).	10
5.	Magnitude of the polarization maximum as a function of wavelength as observed on repeated scans of the sky at Mauna Loa on March 25, 1973.	12
6.	Magnitude of the polarization maximum as observed at $\lambda = 0.60\mu\text{m}$ for different scans of the sun's vertical at Mauna Loa on the dates indicated.	13
7.	Magnitude of the polarization maximum as observed at $\lambda = 0.32\mu\text{m}$ for different scans of the sun's vertical at Mauna Loa on the dates indicated.	14
8.	Magnitude of the polarization maximum at $\lambda = 0.32\mu\text{m}$ versus sun elevation as observed on various dates at Mauna Loa.	17
9.	Magnitude of the polarization maximum at $\lambda = 0.60\mu\text{m}$ as a function of sun elevation as observed on various dates at Mauna Loa.	18

List of Figures (Cont.)

Figure		Page
10.	Angular distance of the Babinet point from the sun for $\lambda = 0.32\mu\text{m}$ versus sun elevation as observed on various dates at Mauna Loa.	19
11.	Angular distance of the Babinet point from the sun for $\lambda = 0.40\mu\text{m}$ versus sun elevation as observed on various dates at Mauna Loa.	21
12.	Angular distance of the Babinet point from the sun versus sun elevation for four different wavelengths as observed at Mauna Loa on March 25, 1973.	22
13.	Angular distance of the Brewster point from the sun versus sun elevation for four different wavelengths as observed at Mauna Loa on March 25, 1973.	23
14.	Normal optical thickness as a function of wavelength at the altitude of the Mauna Loa Observatory for a Rayleigh atmosphere.	25
15.	Degree of polarization as a function of angle in the sun's vertical as observed on Mauna Loa at a wavelength of $\lambda = 0.40\mu\text{m}$ and as computed for a Rayleigh atmosphere of optical thickness $\tau = 0.25$ with surface albedo of $A = 0$ and 0.80 .	27
16.	Degree of polarization as a function of angle in the sun's vertical as observed on Mauna Loa at a wavelength of $\lambda = 0.80\mu\text{m}$ and as computed for a Rayleigh atmosphere of optical thickness $\tau = 0.02$ with surface albedo of $A = 0$ and 0.80 .	29
17.	Degree of polarization of skylight as observed at $\lambda = 0.32\mu\text{m}$ on Mauna Loa (plotted points) and as given by the parameterization algorithm Eq. (6) (solid line). Values of the derived parameters, together with their probable error, are tabulated in the inset.	32

List of Figures (Cont.)

Figure		Page
18.	Values of parameter A_1 as a function of wavelength for various scans of the sky at Mauna Loa on March 25, 1973. (--- forenoon; — afternoon).	33
19.	Values of parameter A_1 at $\lambda = 0.32\mu\text{m}$ as a function of sun elevation for observations at Mauna Loa on the dates indicated.	34
20.	Values of parameter A_1 at $\lambda = 0.50\mu\text{m}$ as a function of sun elevation for observations at Mauna Loa on the dates indicated.	36
21.	Values of parameter A_2 as a function of wavelength for observations at Mauna Loa on March 25, 1973.	37
22.	Values of parameter A_3 as a function of wavelength for observations at Mauna Loa on March 25, 1973. (--- forenoon; — afternoon).	39
23.	Schematic diagram showing the main components of skylight incident at the Mauna Loa Observatory. (I_p : intensity due to primary scattering of direct sunlight by the atmosphere; I_m : intensity due to multiple scattering by the atmosphere; I_c : intensity due to reflection by clouds; I_s : intensity due to reflection by the sea surface.	41

Polarization of Skylight at an Altitude of
11,200 Feet on Mauna Loa, Hawaii

K. L. Coulson, R. L. Walraven, L. B. Soohoo

I Introduction

The degree of polarization of light from the sunlit sky has been found in the past to be a sensitive indicator of the presence of dust, haze, and other types of particles in the atmosphere. The magnitude and distribution of skylight polarization were both strongly affected by volcanic ash injected into the atmosphere by the eruptions of Krakatao on the island of Java in 1883 and the Alaskan volcano Mt. Katmai in 1912. More recent measurements by Dorno (1919), Jensen (1942), Neuberger (1950), Sekera et al (1955), Pyaskovskaya-Fesenkova (1960), Coulson (1971), and others have verified the sensitivity of various parameters of the polarization field to atmospheric turbidity.

One of the sources of concern regarding man's activities is the extent to which he is causing an increase of the particulate content of the atmosphere as a whole. Present evidence on the point is conflicting. In some areas of the world, there are strong indications that atmospheric turbidity is increasing at a rapid rate, whereas observations in other areas indicate a stable condition of particles in the atmosphere.

Of the several atmospheric monitoring stations now being established in various parts of the world, none, as far as is known, is equipped with instruments for measuring the polarization of skylight. Thus it was thought desirable to make a start in this direction by some short term and preliminary measurements at one of the regular monitoring stations. The Mauna Loa Observatory on the island of Hawaii was chosen for the purpose. The rationale behind the choice is that Mauna Loa has a long record of measurements of atmospheric conditions, that multi-spectral measurements of the direct and diffuse solar radiation are available at the site, and that its location is not too remote from California. In addition, the altitude of the Observatory (approximately 11,200 feet MSL) assures that it is in the clear air above the trade wind inversion of the Hawaii area, and it is relatively remote from any local sources of pollution.

II Instrumentation and Operational Procedures

The instrument used for skylight measurements on Mauna Loa is a dual-channel polarizing radiometer which was developed on the Davis Campus of the University of California. It has been briefly described by Coulson and Walraven (1972). Basically, the instrument measures the relative intensity, degree of linear polarization, and the orientation of the plane of polarization of the incident light in any of eight different wavelength ranges from the ultraviolet, through the visible, and into the near infrared regions of the spectrum.

For this rotating analyzer type of polarimeter, the intensity $I(\psi)$ falling on the detector at analyzer angle ψ is, aside from instrumental constants, given by

$$I(\psi) = I_e \cos^2 \psi + I_r \sin^2 \psi + \frac{1}{2} U \sin 2\psi \quad (1)$$

where I_e and I_r are the intensity components along the vertical and horizontal directions, respectively, and U is the Stokes parameter defining the orientation of the plane of polarization x by the relation

$$U = (I_r - I_e) \tan 2x \quad (2)$$

Thus, in theory, the three unknowns (I_e , I_r , U) can be determined from measurements at three different values of ψ . Once these quantities are determined, the total intensity I , degree of polarization P and orientation angle x of the plane of polarization can be computed from Eq. (2) together with the relations

$$I = I_e + I_r \quad (3)$$

$$P = \frac{[(I_e - I_r)^2 + U^2]^{1/2}}{I} \quad (4)$$

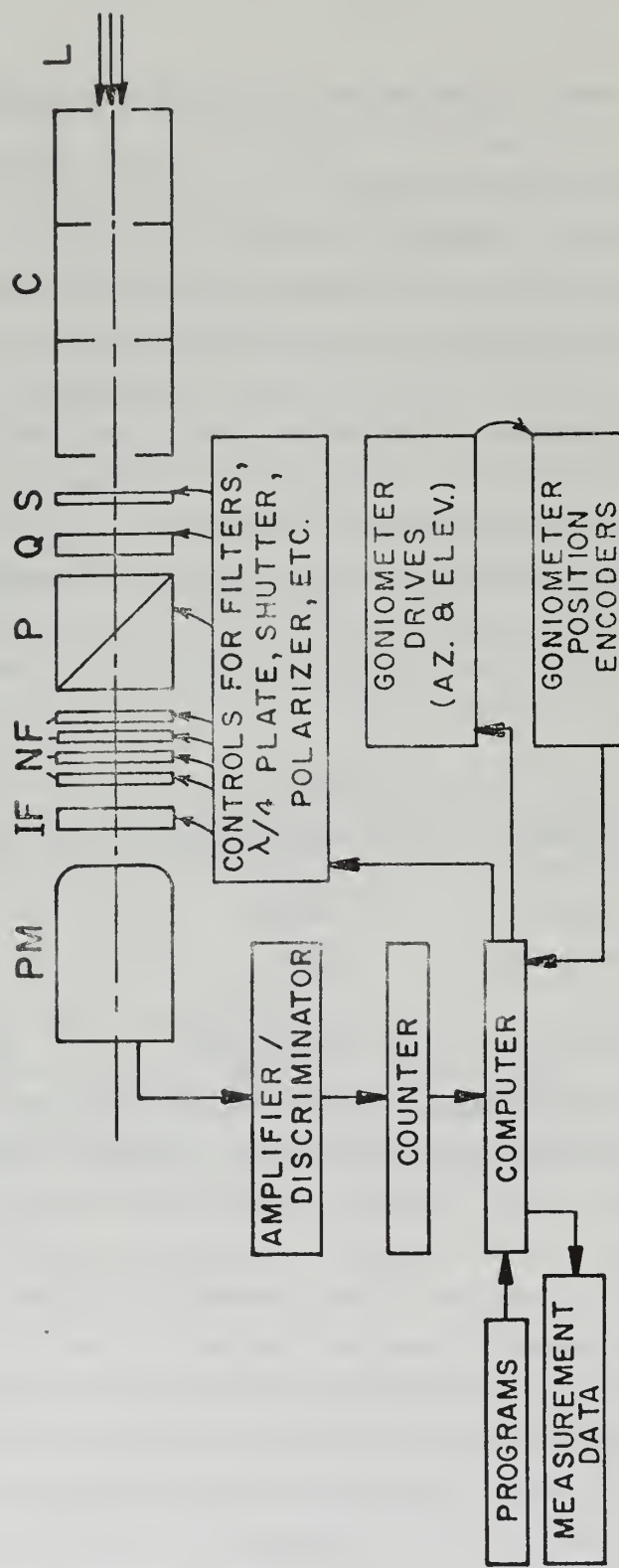
The physical quantities can, in principle, be determined by measurements at three different analyzer angles. However, if corrections are to be made for small stray reflections within the instrument and for drifts in the measured intensity over the time of the measurements, then measurements at six different analyzer angles must be made. It was more convenient, in fact, to determine the physical quantities by a set of eight measurements where the analyzer was rotated 45 degrees between each measurement. These eight values were harmonically analyzed on a real-time basis by the computer and the values of the physical quantities were printed out immediately. The raw data, however,

were stored on magnetic tape for use in possible further processing of the results.

The design of each of the two channels of the polarizing radiometer is shown schematically in Fig. 1. Radiation confined to a 0.75° half-angle cone enters the collimator tube and is transmitted successively through the rotating polarizer (Glan-Thompson prism), an appropriate number of neutral density filters, an interference color filter, and finally it impinges on the photocathode of a photomultiplier tube. The opaque shutter is normally out of the optical path, but it is inserted into position for obtaining a dark count at selected times during instrument operation. The quarter wave plate can be inserted and removed from the optical path as necessary to measure the ellipticity of the incident light stream, but ellipticity was not included in these measurements. Pertinent data on each of the two channels of the instrument are tabulated as follows:

	Channel A	Channel B
Wavelengths of peak transmission of interference filters (μm)	0.32,0.365,0.4.0.5	0.6,0.7,0.8,0.9
Type of photomultiplier tube	EMI6256A	EMI9559A
Central wavelength of quarter wave plate (μm)	0.40	0.70
Type of amplifier discriminator	SSRI Model 1120	SSRI Model 1120

In order to gain the advantages of excellent stability and linear response, coupled with a high signal-to-noise ratio, variable integration time, and direct digital output, photon counting techniques were selected over the conventional analog signal type of system. In a photon counting configuration such as this, the relative precision of measurement is inversely proportional to the square root of the number of photons counted, so there is a simple trade-off between the precision of the data and the speed at which they are taken. For instance, by making photon counts at eight points in one rotation of the polarizer with a one-second integration time at each point, the probable error in the intensity measured by this instrument is $\pm 0.15\%$, that in the magnitude of the degree of polarization is ± 0.002 , and the probable error in the angle of the plane of polarization is $\pm 0.1^\circ$. This was the case for most of the data taken at Mauna Loa. If the integration time at each point had been decreased to 0.1 sec., the rate of data acquisition would have been



L : INCIDENT LIGHT P : ROTATING POLARIZER
 C : COLLIMATOR TUBE NF : NEUTRAL FILTERS
 S : OPAQUE SHUTTER IF : INTERFERENCE FILTER
 Q : QUATER-WAVE PLATE PM : PHOTOMULTIPLIER

Fig. 1 Schematic diagram of one of the two channels of the photon-counting polarizing radiometer.

increased somewhat, but the probable errors would have increased to $\pm 0.5\%$, ± 0.007 , and $\pm 0.3^\circ$ for intensity, degree of polarization, and angle of the plane of polarization, respectively. Although these errors are not excessive, the higher precision mode of operation was generally selected.

The mechanical operation of the instrument, including positioning in azimuth and elevation, changing of filters, rotation of polarizer, etc., is controlled completely by a mini-computer (PDP-11/20), which is an integral part of the system. By appropriate computer programs, any type of scan pattern and measurement sequence can be achieved. This feature provides great flexibility and reliability in the operation, with minimal effort by a human operator. In addition, the signals from the instrument are processed and the required computations performed by the computer to give the output directly in terms of the physical variables of intensity, degree of polarization, and angle of the plane of polarization, all within one second after the measurement is made. Not only does this eliminate the slow and laborious step of data processing, but it also permits immediate inspection of the data to detect any possible malfunction of the system itself.

Skylight measurements on Mauna Loa were made mainly during February and March, 1973. Operational difficulties coupled with a certain number of system malfunctions resulted in somewhat fewer measurements than had been anticipated, but, as will be seen below, the data are more than sufficient to delineate major changes of the polarization field which occurred at that location. Furthermore, processing and analysis of the relatively large number of data which were obtained put a strain on available financial resources to the point that it would not have been feasible to handle more measurements if they had been taken.

The normal operational procedure for making the measurements was to scan the sky in the plane of the sun's vertical (vertical plane through the sun), beginning and ending the scan at 5° above the horizon in the solar and anti-solar azimuths. Data points were taken at regular intervals of sometimes 2° and sometimes 5° throughout the 170° scan, and the two channels of the instrument were operated simultaneously. Thus measurement of relative intensity, degree of polarization, and orientation of the plane of polarization were made in two wavelengths at either 35 or 86 angles in the plane during each scan of the sky. For points at 2° intervals, the scan required approximately 30 minutes, whereas about half of that time was required for 5° data points.

III Results of Measurements

Measurements of skylight polarization were made on Mauna Loa only under conditions of essentially cloudless skies. There were short periods of time when a few wisps of cloud appeared, but appreciable cloudiness in the upward hemisphere was sufficient to stop the measurements. Cumulus type clouds were very common, of course, over the ocean around the island, but these were mainly confined to levels below the trade wind inversion and generally remained below the observation site. There were occasions when the upslope wind brought significant cloud masses over the observatory, but persistent cloud intrusions caused suspension of the measurements.

One difficulty with skylight measurements at Mauna Loa was occasioned by the several antennae and supporting wires projecting above the observation platform. A considerable number of spurious data points resulted from such obstructions in the field of view of the instrument, and since the distribution of the obstructions is very irregular, it is impossible to determine just which of the data points are affected. This is perhaps more of an annoyance than a substantive deficiency in the data, but it is a feature to be considered in possible future measurements.

Since the number of data obtained in the three months period on Mauna Loa is large, it is not feasible to reproduce them all in this report. Consequently a selection has been made to show typical results of complete scans of the sky, the variation and some of the extremes of the polarization field, and the behavior of the polarization maximum and neutral point positions as indicators of changing atmospheric conditions. Finally, a method of parameterization of the data is given, by which most of the essential information of the data can be represented in terms of four simple parameters. It is anticipated that this, or a similar type of representation, will greatly simplify the processing and analysis of polarization data in future studies of atmospheric turbidity.

A. Typical Polarization Distribution

The general distribution of the degree of polarization in the plane of the sun's vertical is shown in Fig. 2. The points shown are the actual data points obtained from the measurements, and no smoothing of the data has been performed. The pattern is generally as expected from computations for a Rayleigh atmosphere (Sekera, 1957). The maximum is located at approximately 90° from the sun, the neutral points (points of $P = 0$) are

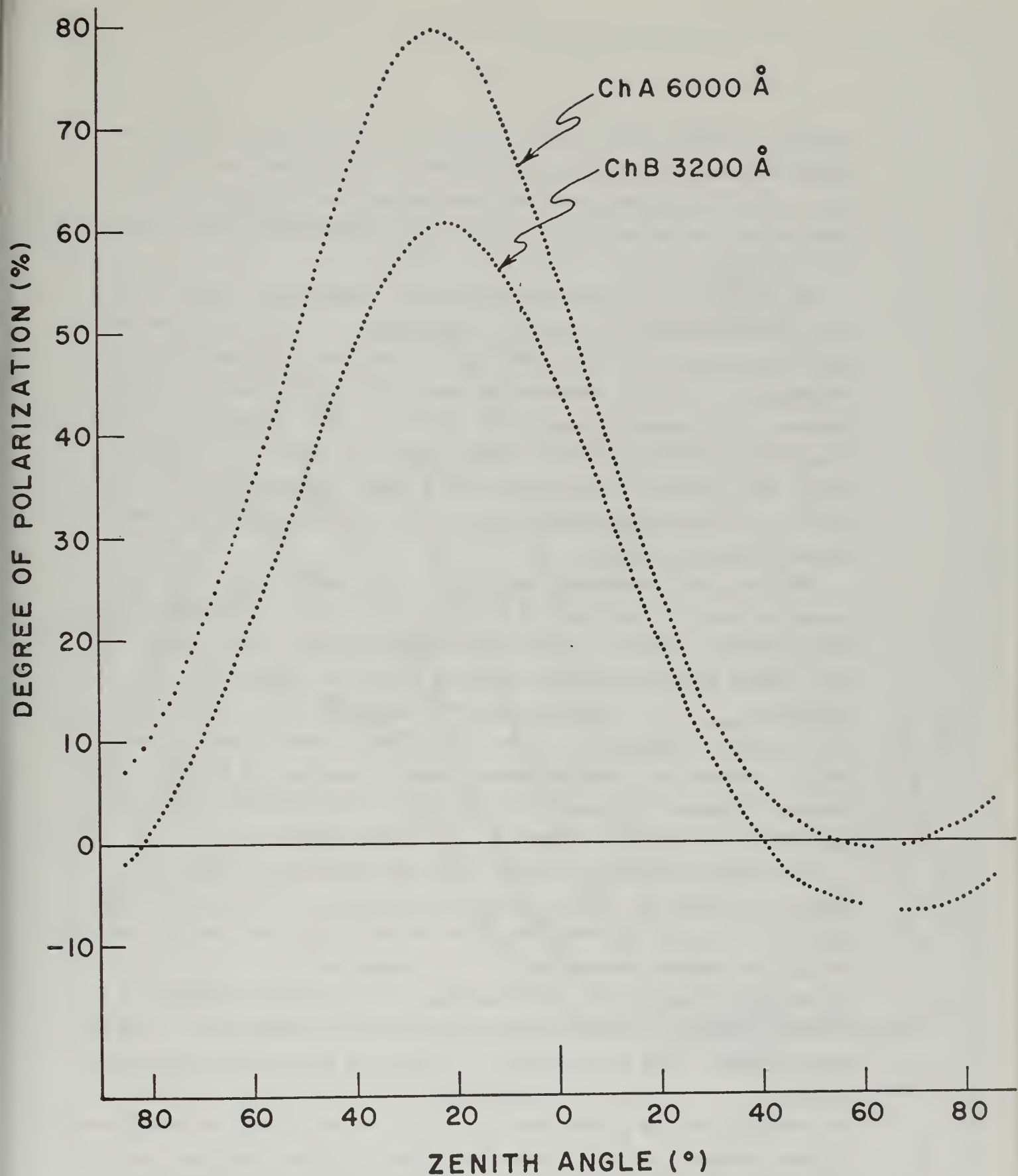


Fig. 2 Typical data on the degree of linear polarization of skylight, as measured by the photon-counting polarizing radiometer. The two channels of the instrument are operated simultaneously for measuring the intensity, degree of polarization, and angle of the incoming radiation. The curves shown are for wavelengths of 0.32 and 0.60 μm , and were obtained during a scan in the plane of the sun's vertical at the Mauna Loa Observatory on February 8, 1973.

located in roughly their normal positions, and the expected strong wavelength dependence is obvious in the curves. Indications that the atmosphere was not purely molecular are seen in the fine structure of the polarization curves and in the neutral points being very close to the sun at $\lambda = 0.60\mu\text{m}$.

The shift of the polarization field with changing sun elevation is shown for wavelengths of 0.32 and $0.60\mu\text{m}$ in Fig. 3. Here also, the maximum of the curves is at about 90° from the sun, and the magnitude P_{max} of the maximum is slightly dependent on zenith angle θ_0 of the sun. These features are as expected from theory (Coulson, 1952). However, P_{max} for a Rayleigh atmosphere reaches a slight minimum at about $\theta_0 = 50^\circ$ to 60° , and no such minimum is seen here at $\lambda = 0.32\mu\text{m}$. There is a tendency for it at $\lambda = 0.60\mu\text{m}$, and it definitely occurs at this wavelength in some of the other Mauna Loa data.

The fact that atmospheric conditions at the mountain site were different on March 25 from those on February 8 can be seen by comparing the data of Figures 2 and 3, even though both were noted as being very clear days. There were more aerosols on March 25 than on February 8. For instance, P_{max} at $\lambda = 0.60\mu\text{m}$ is only 70% or less in Fig. 3, whereas it is 80% in Fig. 2. Similarly, P_{max} at $\lambda = 0.32\mu\text{m}$ is lower in Fig. 3 than in Fig. 2, although by a smaller absolute amount than for $\lambda = 0.60\mu\text{m}$. A similar difference in atmospheric conditions can be deduced from the disappearance of the neutral points at $\lambda = 0.60\mu\text{m}$ on March 25.

It is found throughout the data that the polarization field at the longer wavelengths at which measurements were made ($\lambda = 0.80$ and $0.90\mu\text{m}$) has a fundamentally different character in the region near the sun than that at the shorter wavelengths. This is shown in Fig. 4. Not only do the neutral points at $\lambda = 0.90\mu\text{m}$ disappear, but the minimum degree of polarization reached for the higher sun elevations is fully 5%. Thus the entire region of the solar aureole is positively polarized at the longer wavelengths. In addition, the magnitude of the polarization maximum is considerably less at $0.90\mu\text{m}$ than at $0.50\mu\text{m}$. In evaluating the significance of these points it should be remembered that for a pure Rayleigh atmosphere overlying a non-reflecting surface, the polarization maximum increases in magnitude with increasing wavelength, and there is always at least one point at which the polarization is zero. Some possible explanations of

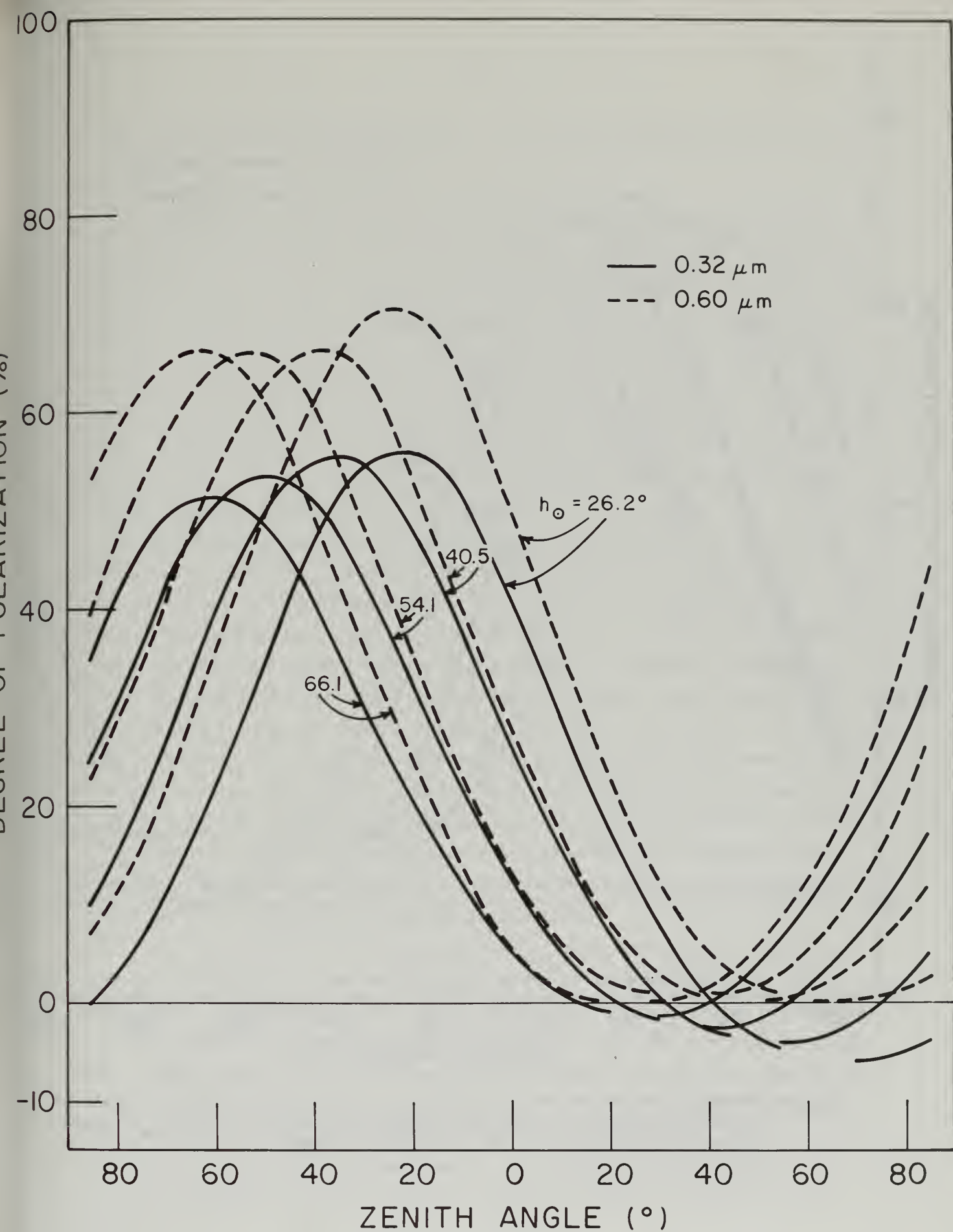


Fig. 3 Degree of polarization of skylight in the sun's vertical as observed in two wavelengths during four different scans of the sky at Mauna Loa on March 25, 1973. ($\lambda = 0.32$ and $0.60\mu\text{m}$).

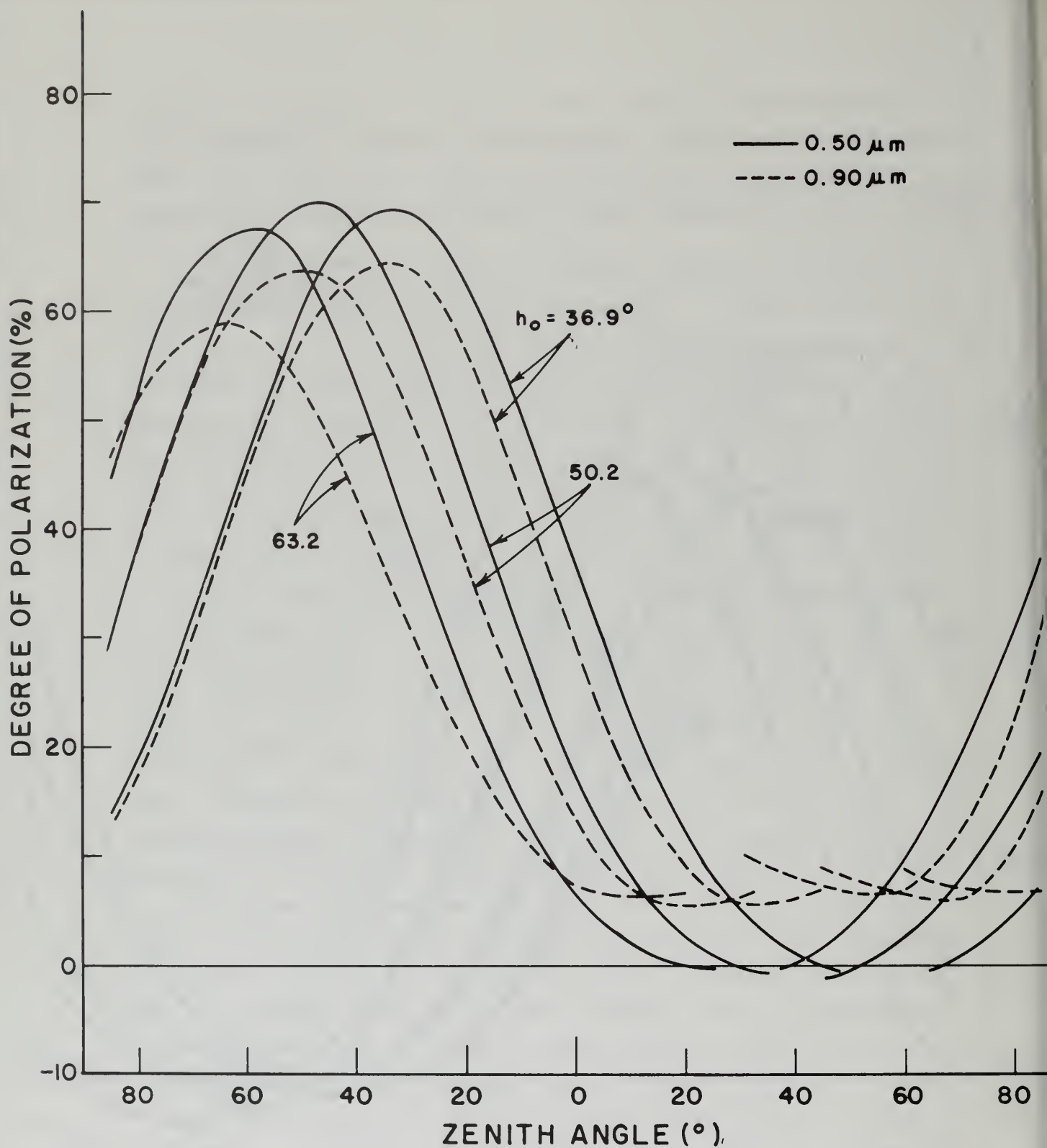


Fig. 4 Degree of polarization of skylight in the sun's vertical as observed in two wavelengths during three different scans of the sky at Mauna Loa on March 25, 1973. ($\lambda = 0.50$ and $0.90\mu\text{m}$).

the apparently anomalous behavior of the actual polarization field are suggested in a later section.

B. Spectral Distribution of the Polarization Maximum

As indicated above, the magnitude P_{\max} of the polarization maximum at Mauna Loa is a relatively strong function of wavelength. A summary of the dependence of P_{\max} on wavelength as obtained on about 25 scans of the sky on March 25, 1973, is shown in Fig. 5. The two groups of data were taken simultaneously by the two channels of the instrument, and the data points from each series of four successive scans of the sky are connected by straight lines. Data for two wavelengths were obtained on each scan, the wavelength pairs for the two channels being 0.32 and 0.60 μm ; 0.365 and 0.70 μm ; 0.40 and 0.80 μm ; and 0.50 and 0.90 μm . Each series of four scans required about one hour to complete.

Although there is a considerable scatter in the data, it is evident from Fig. 5 that P_{\max} reaches a maximum in the 0.50 to 0.60 μm range. The lower values at shorter wavelengths are expected from computations for a molecular atmosphere, in which case the decrease of polarization values with decreasing wavelength is mainly a result of multiple scattering by the atmospheric gases. However, multiple scattering cannot explain the decrease P_{\max} with increasing wavelengths beyond $\lambda = 0.60\mu\text{m}$, and in fact progressively decreasing multiple scattering with increasing wavelength would indicate the opposite trend. Thus the explanation of the behavior of P_{\max} in the longer wavelength range must be an increasing influence of non-Rayleigh effects, the most important being aerosol scattering and surface reflection. The relative contributions of these two effects is difficult to estimate from present information.

The variations of the magnitude of P_{\max} with time, on both hour-to-hour and day-to-day time scales, were found to be unexpectedly large on Mauna Loa. A summary of the variations on all of the days for which data are available is given for $\lambda = 0.60\mu\text{m}$ in Fig. 6 and for $\lambda = 0.32\mu\text{m}$ in Fig. 7. There appears to be some systematic variation in the data, the values in January, February, and the last days of March being relatively high, and the period March 12-25 showing generally lower values. To the extent that this variation is representative, it would indicate a period of increased turbidity of the atmosphere from the middle to near the end of March.

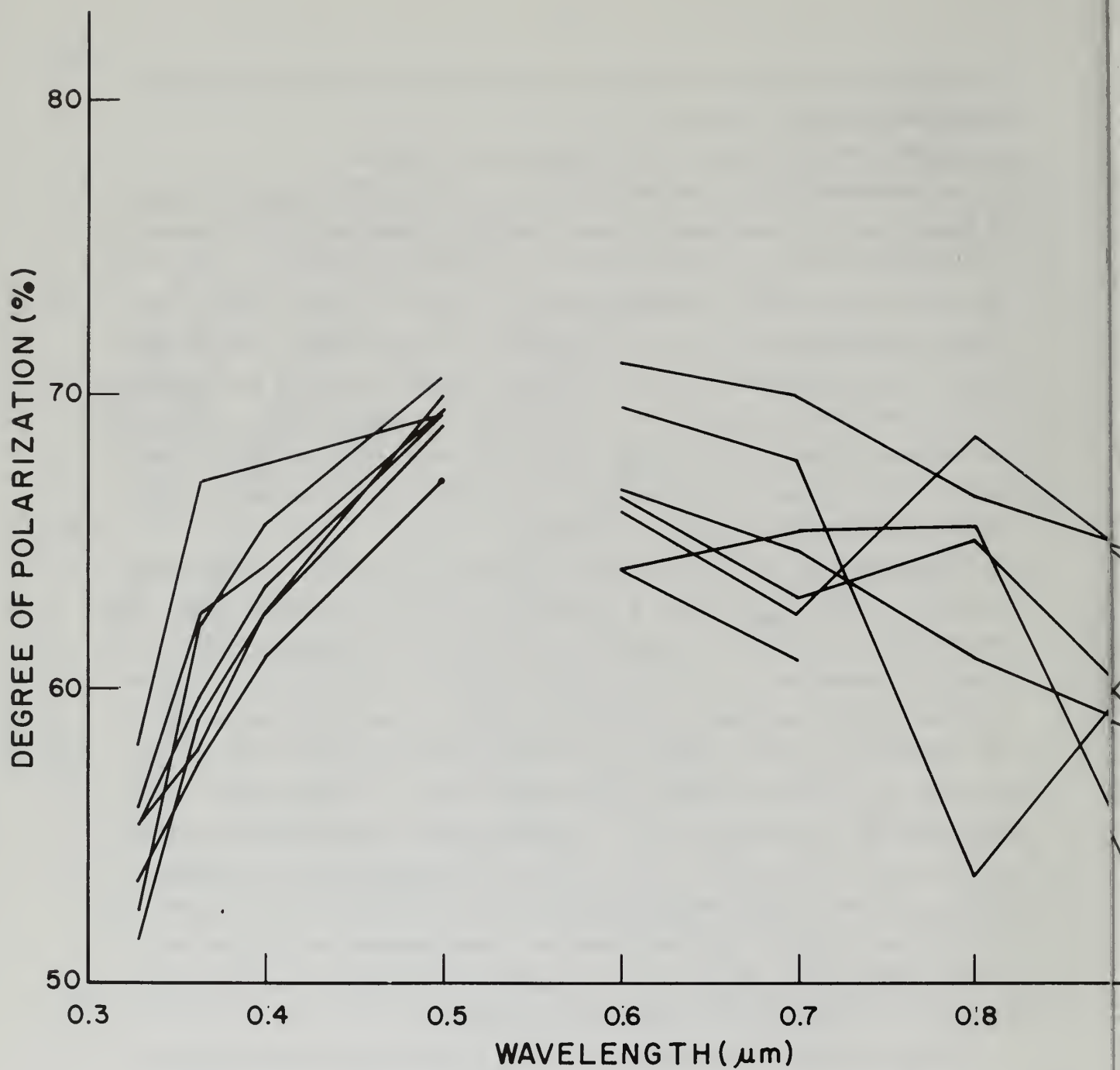


Fig. 5 Magnitude of the polarization maximum as a function of wavelength as observed on repeated scans of the sky at Mauna Loa on March 25, 1973.

POLARIZATION MAXIMUM (%)

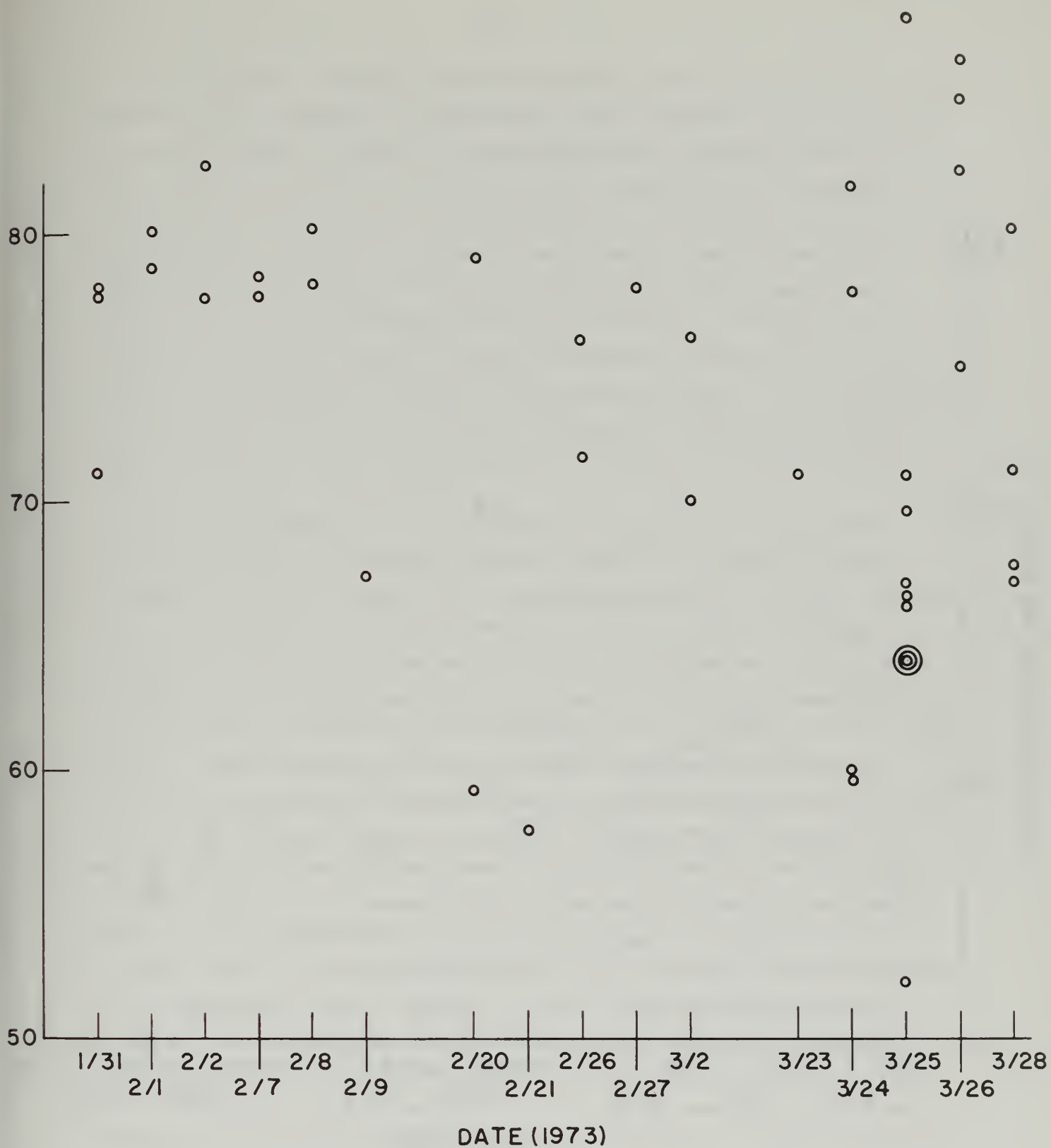


Fig. 6 Magnitude of the polarization maximum as observed at $\lambda = 0.60\mu\text{m}$ for different scans of the sun's vertical at Mauna Loa on the dates indicated.

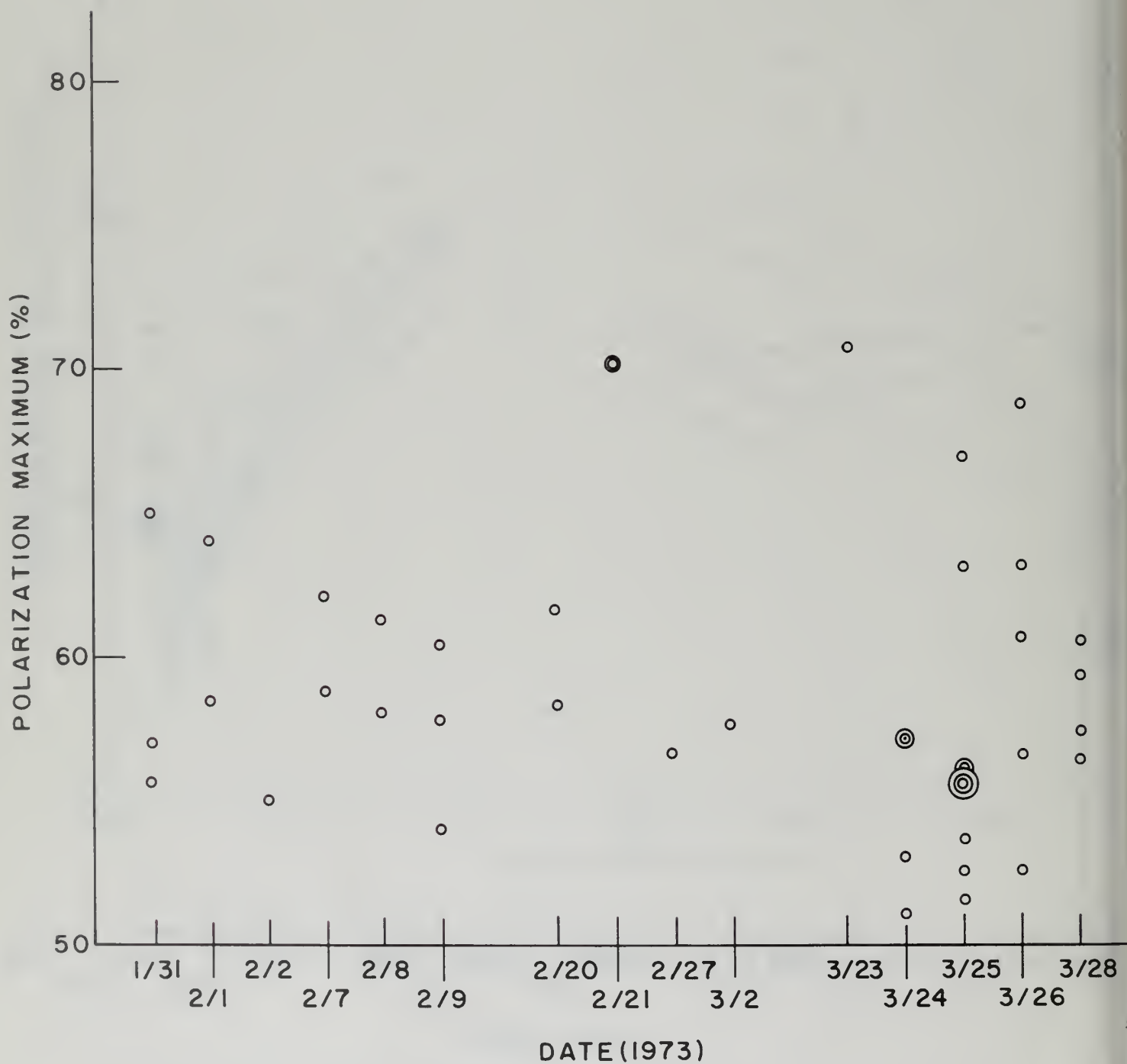


Fig. 7 Magnitude of the polarization maximum as observed at $\lambda = 0.32\mu\text{m}$ for different scans of the sun's vertical at Mauna Loa on the dates indicated.

It is obvious, however, that the variations within the period of a single day are comparable in magnitude to those observed over longer time intervals. Since the time of observations was not consistent from day to day and more afternoon observations were taken in the March 22-25 period than at other times, it is possible that the apparent trends in P_{\max} are due to biases in the time of measurement. For instance, the data of March 25, which are the most complete data taken, show lower values of P_{\max} in the afternoon than in the forenoon. Presumably the afternoon decrease is caused by higher atmospheric turbidity brought to the top of the mountain by upslope winds which developed in the afternoon. If this diurnal pattern was prevalent during other observational periods, then the apparent trends are probably the result of a time bias in the data.

The large magnitude of the variations of P_{\max} is one of the most puzzling features of the Mauna Loa data. While it is known that the polarization field is sensitive to atmospheric conditions, one would think that the atmosphere at Mauna Loa would be stable enough to yield only small variations of the polarization field. An indication that this is not the case was already seen by Dr. R. Hansen and his colleagues (private communication) in connection with their Mauna Loa observations of the solar corona. Large variations of the polarization component introduced by scattering in the earth's atmosphere were frequently observed to occur near the disk of the sun. These perturbations covered periods ranging from minutes to hours, and did not appear to be correlated with obvious atmospheric changes. Since Hansen's observations were confined to the region near the sun, no information on the variability of the polarization field in other parts of the sky was available until the present series of polarization measurements was initiated. In fact, the observations are still inadequate to establish a correlation between variations very near the sun and those of other parts of the polarization field, although a strong correlation would not be unexpected. It is likely that the entire polarization field responds to whatever changes of atmospheric optical properties which occur.

The variation of the polarization maximum P_{\max} with sun elevation derived from all of the measurements taken at Mauna Loa is shown for

$\lambda = 0.32\mu\text{m}$ in Fig. 8 and for $\lambda = 0.60\mu\text{m}$ in Fig. 9. Although there appears to be a trend toward decreasing polarization with increasing sun elevation, the striking feature of these diagrams is the great variability of P_{max} . Variations of 10% or more occur frequently with relatively small changes of sun elevation on a single day at $\lambda = 0.32\mu\text{m}$. At $\lambda = 0.60\mu\text{m}$ the short period variations are less pronounced than at the shorter wavelength, but there is still a large amount of scatter in the data. Other wavelengths show a similar behavior of P_{max} . As discussed more fully below, the large variability is thought to be brought about by a combination of optical instability of the atmosphere and changing reflection from the clouds and sea surface surrounding the island.

C. Positions of the Neutral Points

Many authors in the past (Soret, 1888; Dorno, 1919; Jensen, 1942; Sekera, 1957; Coulson, 1971; Neuberger, 1950; and others) have found the positions of the three neutral points (Babinet, Brewster, and Arago) to be relatively sensitive to atmospheric turbidity. The positions, however, are somewhat difficult to determine very precisely because of the low magnitudes of the polarization in their vicinity. Residual polarization of very minor amounts introduced by the polarimeter itself can cause significant errors in absolute determinations of the neutral point positions, although relative changes can be delineated very well if the observations are all made with the same instrument. In the present case, the probable error in determinations of the absolute positions of the neutral points is estimated to be about 3° , while the relative error is perhaps half that. Another difficulty in studies of neutral point behavior is that the Babinet and Brewster points become very close to the sun, and the Arago point close to the anti-sun, in the $0.60 - 0.70\mu\text{m}$ region, and they disappear completely at $0.80 - 0.90\mu\text{m}$. Because of these features, emphasis in the present study has been in the $0.32 - 0.50\mu\text{m}$ spectral region.

The angular distance between the Babinet point at $\lambda = 0.32\mu\text{m}$ and the sun is shown as a function of sun elevation in Fig. 10 for all of the measurements taken at Mauna Loa. There is an obvious dependence of the position on sun elevation, as is expected on the basis of molecular scattering (Coulson, 1952). Superimposed on this dependence, however, is a large variability of the values in which there appears to be some

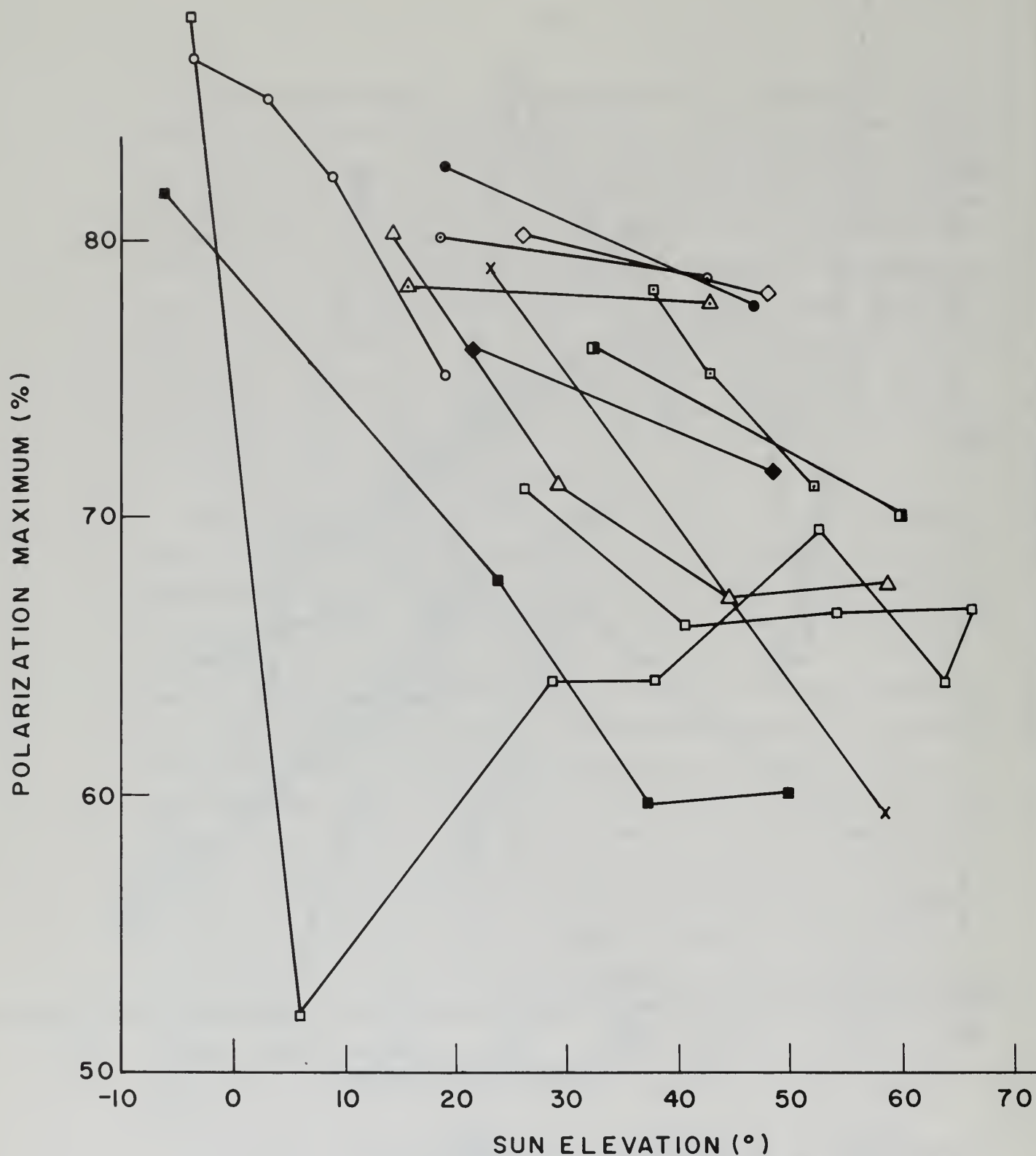


Fig. 9 Magnitude of the polarization maximum at $\lambda = 0.60\mu\text{m}$ as a function of sun elevation as observed on various dates at Mauna Loa.

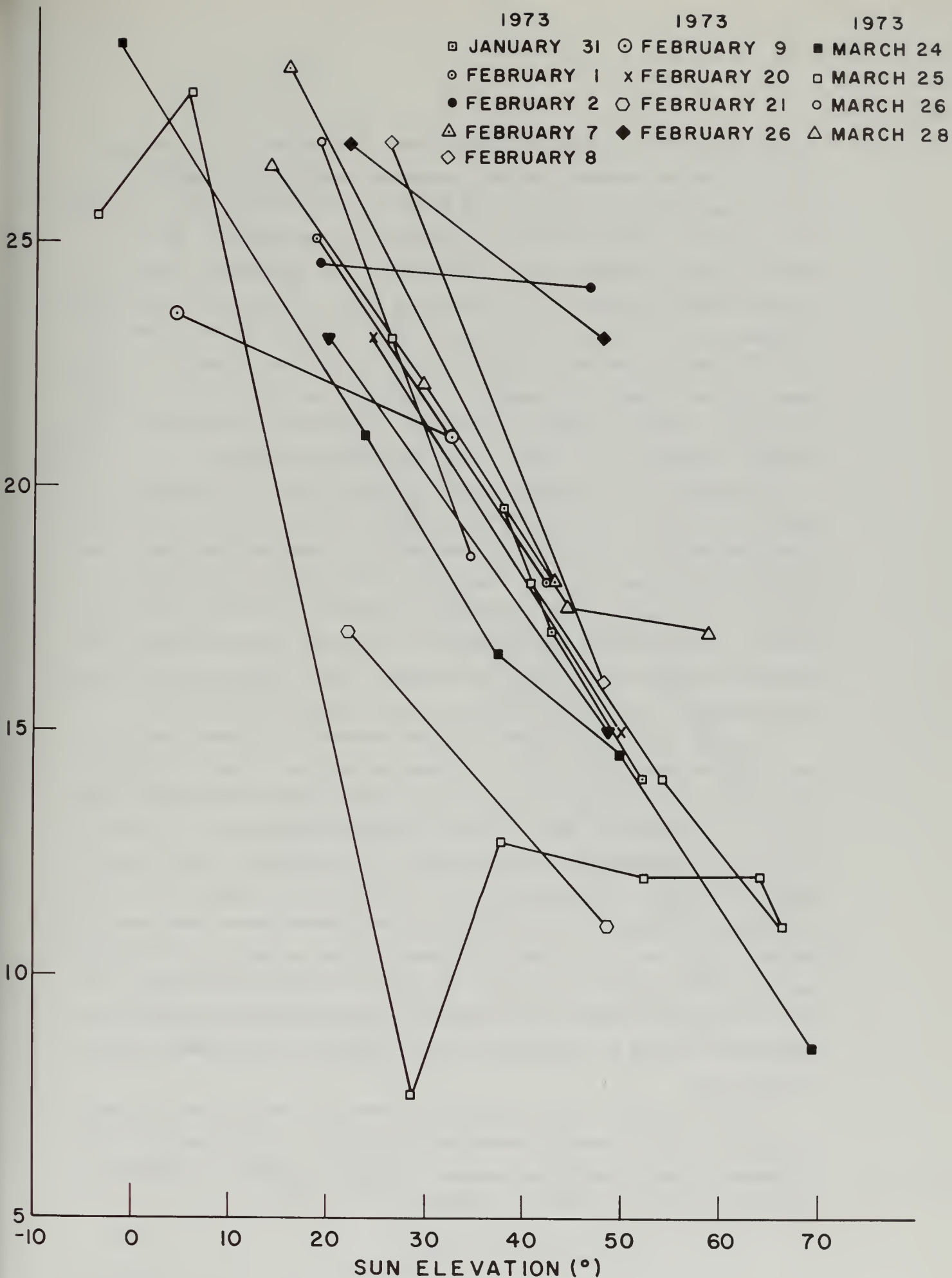


Fig. 10 Angular distance of the Babinet point from the sun for $\lambda = 0.32\mu\text{m}$ versus sun elevation as observed on various dates at Mauna Loa.

consistency. For instance, the conclusion was reached on the basis of the polarization maximum that the atmosphere was optically unstable on March 25 and that the turbidity was greater during the afternoon than in the forenoon. This conclusion is supported by the behavior of the Babinet point, as shown in Fig. 10 through a very significant shift of the point toward the sun in the afternoon hours. A similar characteristic is shown for $\lambda = 0.40\mu\text{m}$ in Fig. 11, in which case the Babinet point is 4 to 5° closer to the sun in the afternoon than in the forenoon. In both cases the data show the atmosphere to have been more turbid in the March 24-25 period than in either the main part of February or on March 28, as already concluded on the basis of the polarization maximum.

The behavior of the Babinet point at four different wavelengths on the optically unstable day of March 25 is shown in Fig. 12. The relatively strong dependence of position on wavelength is expected from theory, as multiple scattering, the main reason for the existence of the neutral points, is strongest at the shortest wavelengths. In each of the wavelengths, however, there is a difference of several degrees between forenoon and afternoon positions of the Babinet point, indicating once again an increase of turbidity with time to have occurred on March 25.

A similar effect is indicated by the Brewster point positions for March 25, as shown by Fig. 13. In interpreting these data it should be realized that the Brewster point, being located some distance below the sun, is not observable until the sun reaches an elevation of 20 - 25°, so that fewer measurements are available for the Brewster point than for the Babinet point. Furthermore, the gradients in the polarization field are generally weaker in the vicinity of the Brewster point than near the Babinet point, so it is likely that observational errors for the Brewster point are the greater of the two. In spite of these difficulties, however, the general shift of the Brewster point toward the sun during the afternoon of March 25 corroborates the conclusion of increased turbidity at that time.

A similar shift of the Arago point toward the anti-sun would normally be expected with increasing atmospheric turbidity. Unfortunately, the measurements available in the present case are too sparse to adequately determine the behavior of the Arago point.

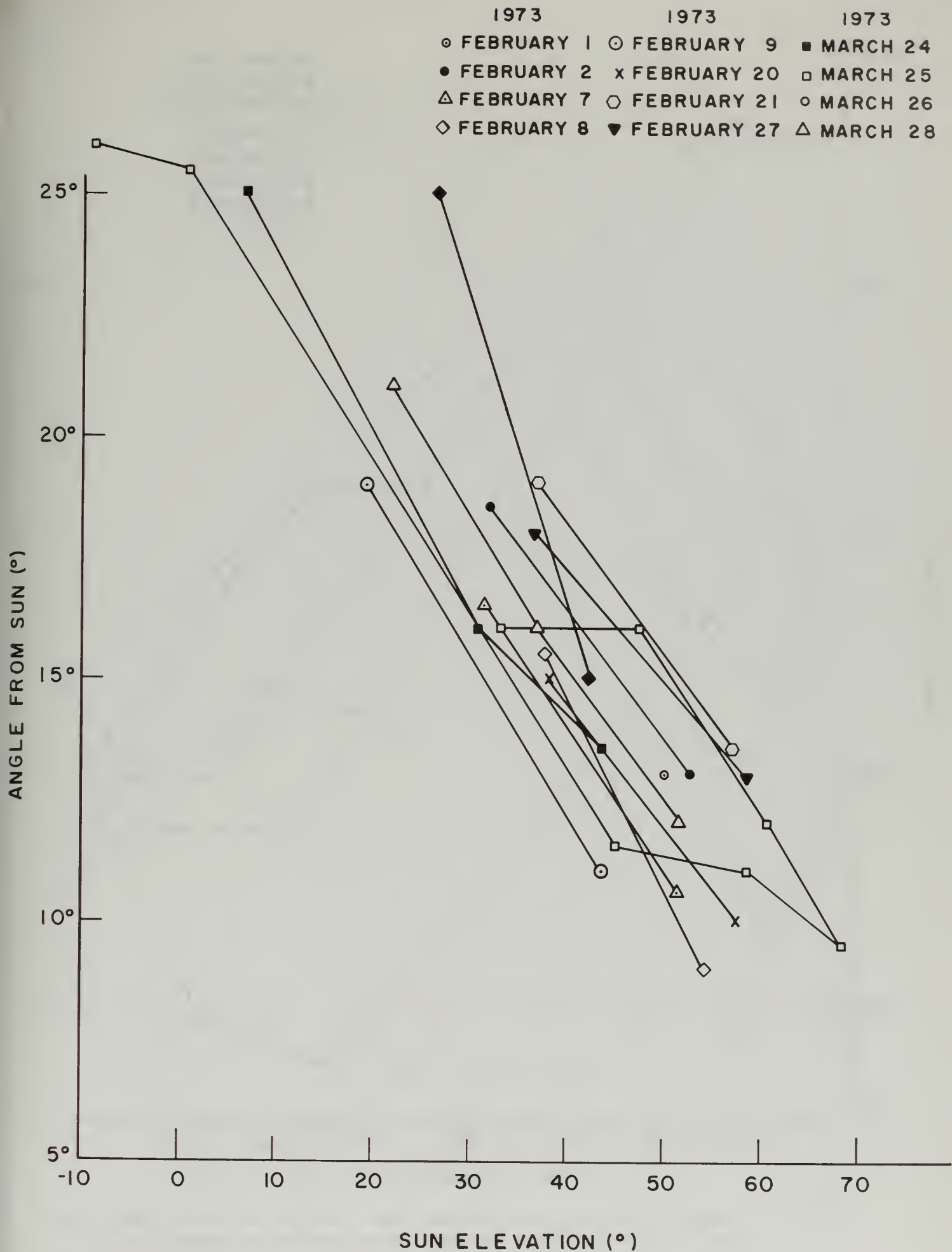


Fig. 11 Angular distance of the Babinet point from the sun for $\lambda = 0.40\mu\text{m}$ versus sun elevation as observed on various dates at Mauna Loa.

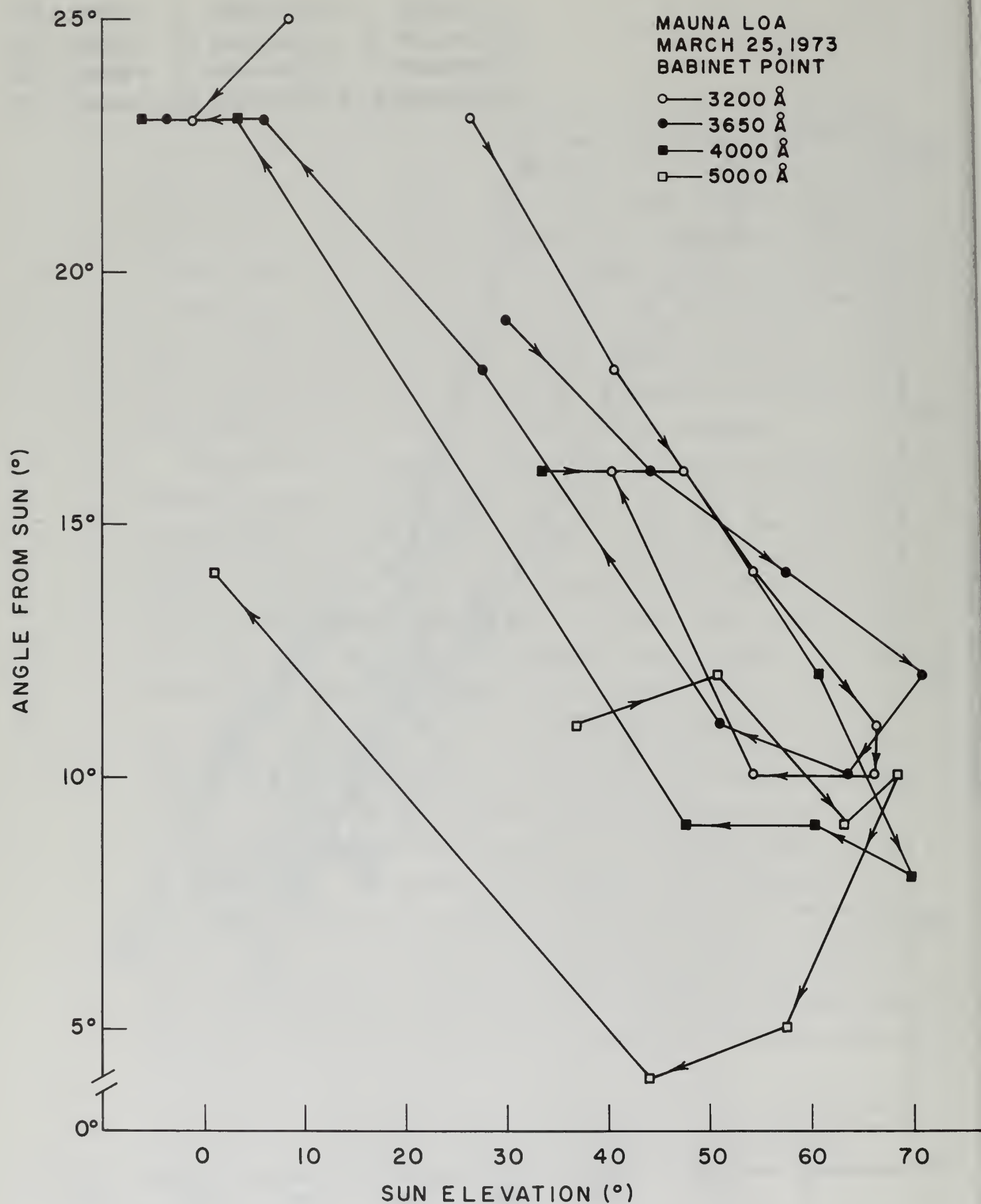


Fig. 12 Angular distance of the Babinet point from the sun versus sun elevation for four different wavelengths as observed at Mauna Loa on March 25, 1973.

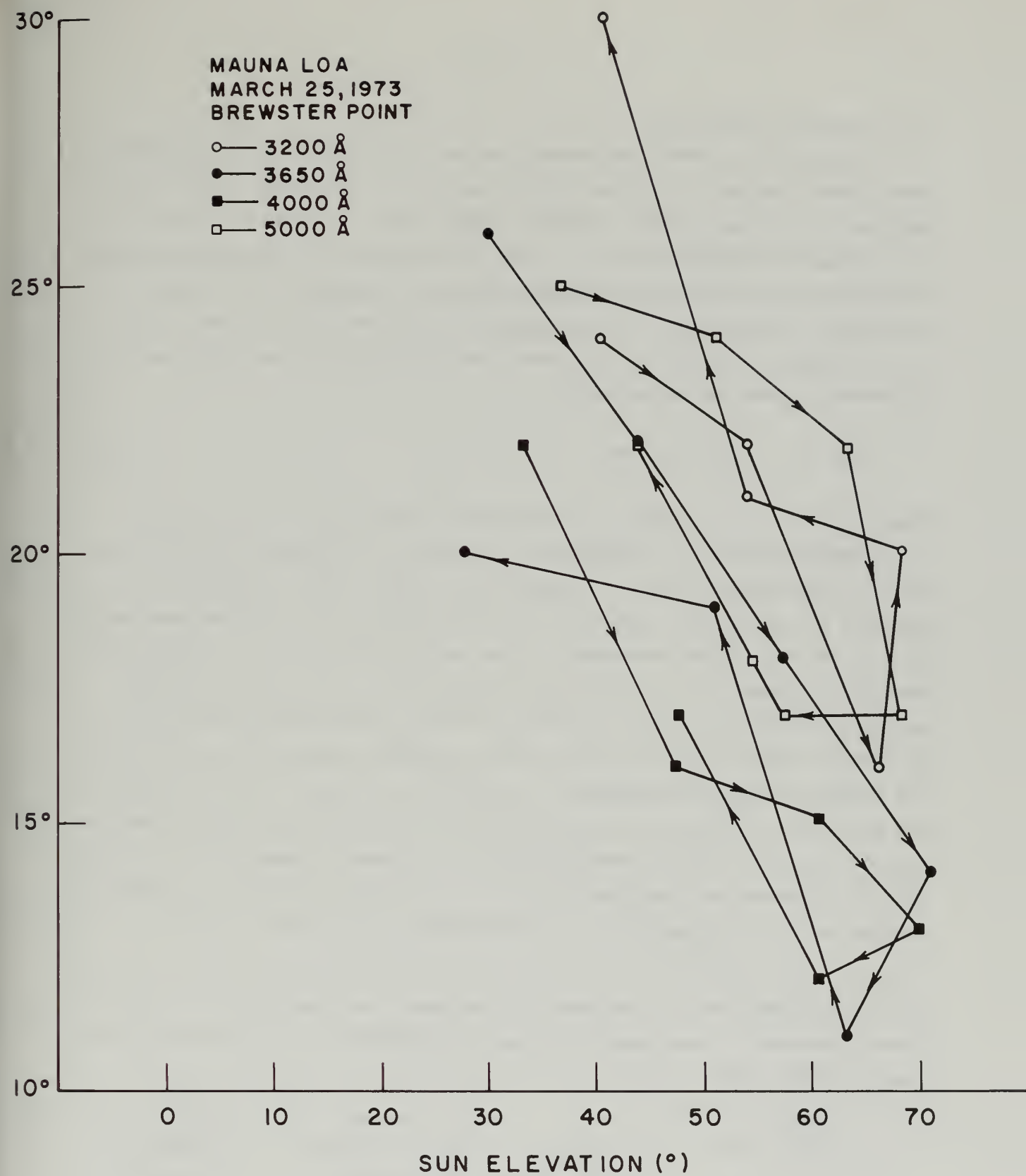


Fig. 13 Angular distance of the Brewster point from the sun versus sun elevation for four different wavelengths as observed at Mauna Loa on March 25, 1973.

IV Comparison with Theory

Because of its very low aerosol content, scattering by the atmosphere above Mauna Loa may, to a first approximation, be considered to follow the Rayleigh scattering model. Existing computations, in which all orders of scattering are considered, may be used for comparing the measurements with theoretical expectations, and thereby gain some insight into the physical mechanisms of importance in determining the observed polarization field.

A primary parameter in the theory of scattering is the normal optical thickness τ given by the relation

$$\tau(\lambda, z) = \int_z^{\infty} \beta(\lambda, z) dz \quad (5)$$

where $\beta(\lambda, z)$ is the volume scattering coefficient of the clear air at a given wavelength and z is height above sea level. The normal optical thickness at an observation site is simply an integration of the scattering effects of all of the air, taken in the zenith direction, from the observation site to the top of the atmosphere. The coefficient $\beta(\lambda, z)$ is a well known function of height for a pure molecular atmosphere. It is thus a simple matter to determine values of optical thickness versus wavelength for the particular observation site, after which available tabulations can be used for comparison with observations. A plot of $\tau(\lambda)$ versus λ for the height of the Mauna Loa Observatory is given as Fig. 14, according to unpublished computations by the authors based on the U. S. Standard Atmosphere. From these data it is determined that the values of $\tau(\lambda)$ at Mauna Loa for the peak wavelengths of the filters used for the measurements are given in Table 1.

Table 1. Normal optical thickness at the Mauna Loa Observatory for a Rayleigh atmosphere at wavelengths of peak transmissions of the optical filters used in these measurements.

$\lambda(\mu m)$	τ	$\lambda(\mu m)$	τ
0.320	0.625	0.600	0.0468
0.365	0.333	0.700	0.0250
0.400	0.246	0.800	0.0146
0.500	0.0982	0.900	0.0091

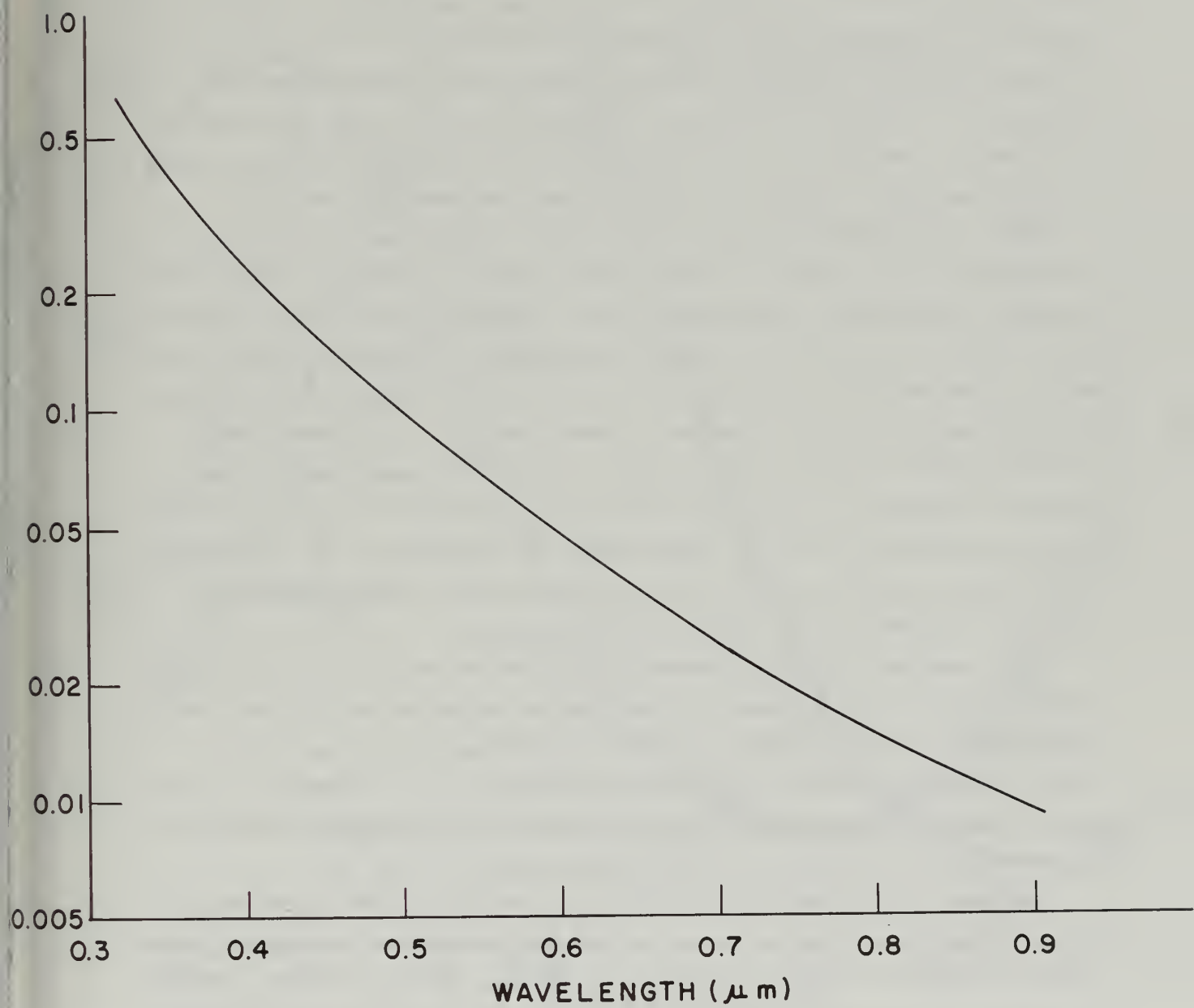


Fig. 14 Normal optical thickness as a function of wavelength at the altitude of the Mauna Loa Observatory for a Rayleigh atmosphere.

Measurements at $\lambda = 0.40\mu\text{m}$ obtained during two sweeps of the sky in the principal plane at Mauna Loa are compared with the polarization in a Rayleigh atmosphere, as tabulated by Coulson, Dave, and Sekera (1960), for two different surface albedos ($A = 0$ and 0.80) in Fig. 15. These measurements, taken on March 25, 1973, are typical of the observational results in general, and were selected so as to correspond relatively closely to sun elevations for which computations are available. In comparing the results it should be realized that the positions of the sun were not identical for the two types of curves, thereby causing a lateral shift of their relative positions, and that there is a slight distortion of the angular position of the observed curves due to the fact that the sun moved a finite angular distance during the approximately 15 minutes required to make one sweep of the sky.

After taking these factors into account, a great deal of similarity is seen between the two sets of curves. Their general shapes are very similar, the negative branches of the curves occur at about the same angles with respect to the sun and are of comparable magnitudes, and the positions of the maxima are at about 90° from the sun. All of these features indicate the Rayleigh character of the atmosphere above Mauna Loa. The most obvious deviation between the two sets of curves is in their magnitudes in the region of the maxima. In view of the very low albedo of the lava surrounding the Observatory site, one might expect the observations to approximate the Rayleigh curves for $A = 0$, but in fact there are approximately 20% difference between them at the polarization maxima.

There are two effects, irrespective of the aerosols in the atmosphere, which contribute to a decrease of the observed polarization. First, the computations do not take into account the molecular anisotropy of the oxygen, nitrogen, and other gases constituting the real atmosphere. This factor would decrease the value at the maximum of the computed curves by approximately 4%, leaving a residual discrepancy of about 16%.

The other major non-aerosol effect for explaining this discrepancy is surface reflection. The fact that surface reflection has a large influence on the polarization field of skylight can be seen by comparing the theoretical curves for $A = 0.80$ with those for $A = 0$. The polarization maximum is decreased by a factor of more than 2 for the case of high albedo. While the albedo of the lava surrounding the Mauna Loa Observatory is low (perhaps 5 to 7%), it is certainly not zero, and this reflected radiation would tend to

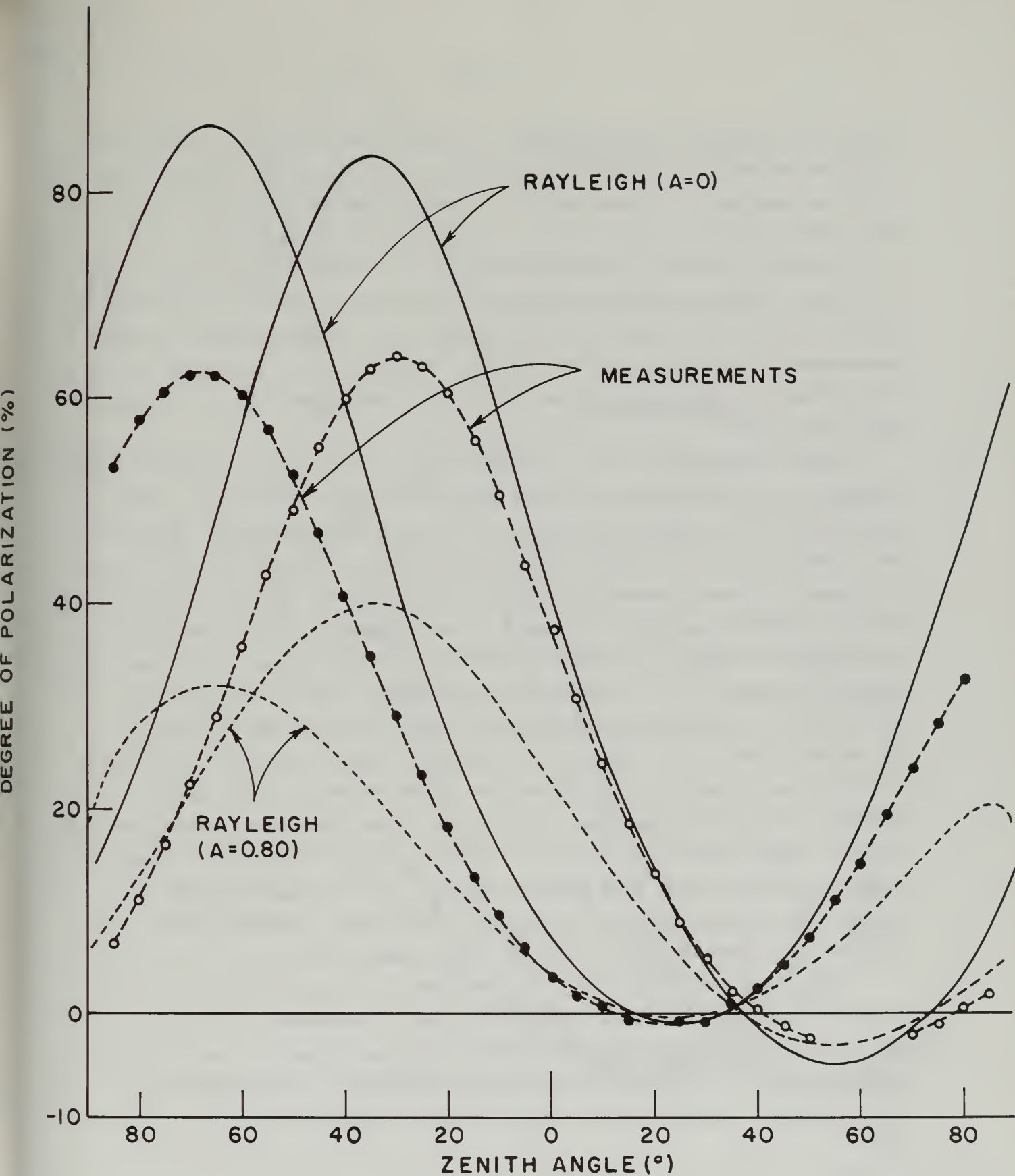


Fig. 15 Degree of polarization as a function of angle in the sun's vertical as observed on Mauna Loa at a wavelength of $\lambda = 0.40\mu\text{m}$ and as computed for a Rayleigh atmosphere of optical thickness $\tau = 0.25$ with surface albedo of $A = 0$ and 0.80 .

decrease the degree of polarization of the sky over the site. In addition, light reflected by other types of surfaces on the island and by clouds and water surrounding the island would tend to increase the effective albedo, and thus further decrease the polarization of the observed skylight.

Finally, of course, are the aerosols in the atmosphere above the observation site. Although the main objective of the measurements was to detect and characterize aerosol effects, it is apparent from these and other data that non-aerosol effects are very important in the Mauna Loa observations and it is difficult to distinguish between the two. This aspect will be discussed more fully below.

Typical measurements at $\lambda = 0.80\mu\text{m}$ are compared with data for a Rayleigh atmosphere at approximately the same optical thickness in Fig. 16. These measurements were taken simultaneously, by the second channel of the polarimeter, with those at $\lambda = 0.40\mu\text{m}$ shown in the previous diagram. There is more discrepancy between observation and theory at $\lambda = 0.80\mu\text{m}$ than at $\lambda = 0.40\mu\text{m}$, the most probable explanation being a larger relative effect of aerosols at the longer wavelength. Rayleigh scattering is very weak due to the small optical thickness at $\lambda = 0.80\mu\text{m}$, and aerosols are correspondingly more effective in determining the polarization field. The most explicit evidence of aerosol effects would seem to be the existence of a positive polarization field in the vicinity of the sun and the strong decrease of the polarization maximum from the Rayleigh case. However, it is not completely clear that the first of these effects may not be due to positive polarization introduced by reflection of the solar beam from the surface of the sea surrounding the island, and the second due to reflections from clouds. Both of these possibilities are considered more fully in the discussion section of this report.

In the interest of brevity, only this brief comparison between the measurements and the theoretical results for model atmospheres is included here. The main types of discrepancy are shown by Figures 15 and 16, and although details vary, the results shown are generally typical of the measurements taken at other wavelengths and times during the observation period at Mauna Loa.

V. Parameterization of the Polarization Field

It is evident from the results given above, as well as from numerous studies in the past, that a large number of measurements, with the attendant

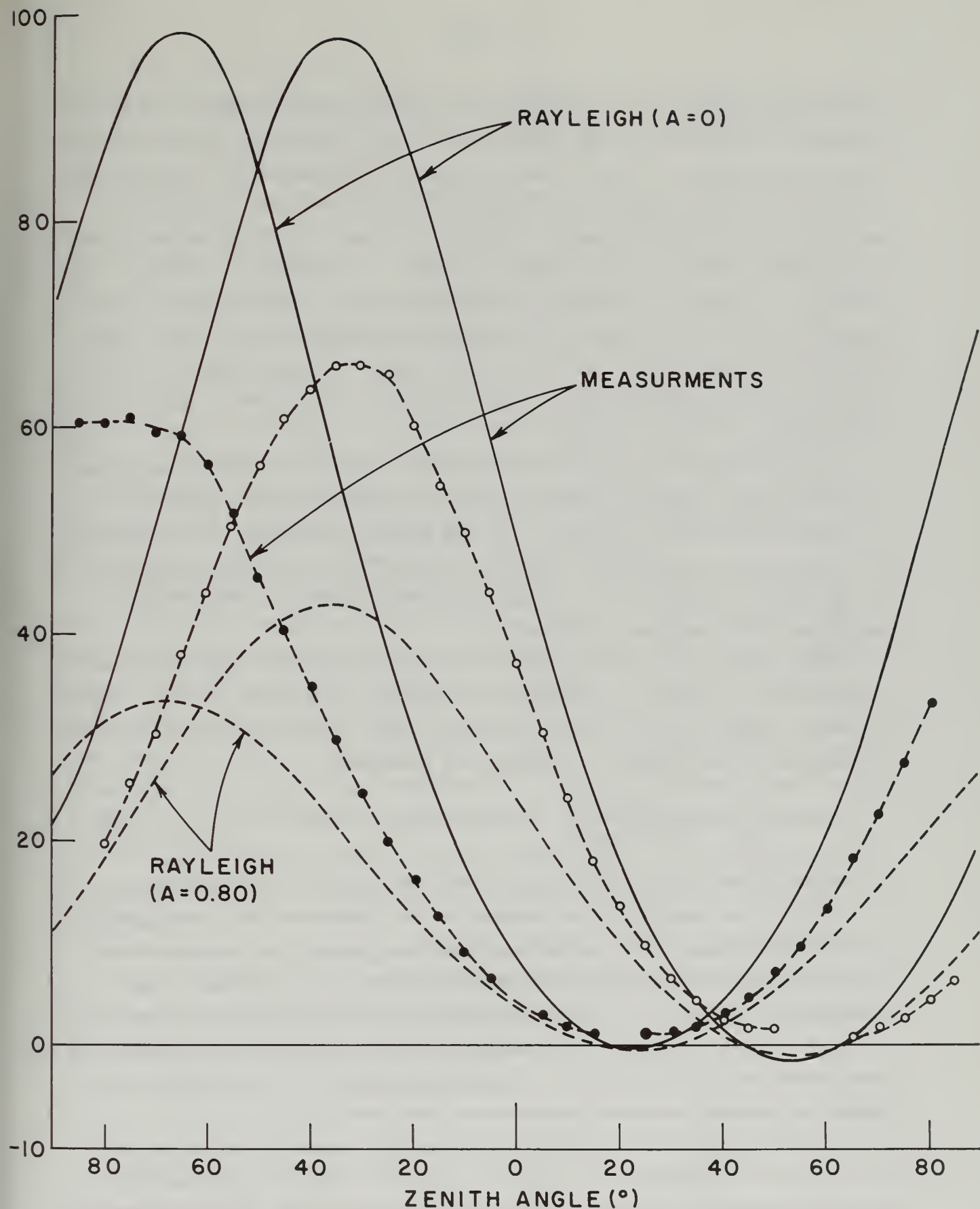


Fig. 16 Degree of polarization as a function of angle in the sun's vertical as observed on Mauna Loa at a wavelength of $\lambda = 0.80\mu\text{m}$ and as computed for a Rayleigh atmosphere of optical thickness $\tau = 0.02$ with surface albedo of $A = 0$ and 0.80 .

problems associated with acquiring and analyzing massive numbers of data, are necessary to characterize the polarization field of skylight by means of the traditional methods. Clearly a more convenient representation, and one with a higher information density, is desirable in any extensive study of the polarization problem. Attempts to develop a parameterization scheme by previous authors have been based almost entirely on an empirical fitting of the data, and any physical interpretation has been lost in the process. For instance, the method developed by Pyaskovskaya-Fesenkova (1958, 1960) and extended by Stamov (1970) has been applied mainly to measurements of the polarization distribution in the solar almucantar, and does not admit a representation of the neutral points.

An effort has been made on the project to develop a somewhat more physically meaningful scheme of parameterizing the polarization distribution in the plane of the sun's vertical. The two prime requirements for the method were taken as (1) providing a representation of the existence and position of the neutral points and (2) giving a parameter closely related to the magnitude of the maximum polarization.

The parameterization algorithm finally developed here, which is based on a combination of physical reasoning and empirical fitting of the data, is the following, where θ is the scattering angle (angle between the directions of propagation of the incident and scattered radiation):

$$P(\theta) = A_1 + A_2 \frac{\sin^2 \theta}{1 + \cos^2 \theta} + A_3 \sin (2\theta) + A_4 \sin (4\theta) \quad (6)$$

The polarization field is then represented in terms of the parameters A_i , $i = 1, 2, 3, 4$, and hopefully the behavior of the parameters with wavelength, sun elevation, atmospheric turbidity, and other physical attributes of the system will permit a simple interpretation of the system by means of the parameters. Unless such an interpretation is possible, then the parameters lose their value by serving no practical purpose. If, however, a reasonable representation is achieved, then a computer, with all its speed and convenience, can be used to assist in analyzing the data.

Although the results of applying the above relation to observational data are still preliminary, it appears possible to fit the observational data reasonably well by means of the four parameters, and that the parameters hold promise of a high correlation with the physical parameters of the system.

Only at the longer wavelengths of the present data ($\lambda = 0.90\mu\text{m}$) does the relationship fail to provide a reasonable representation of the distribution of polarization in the principal plane.

A typical fit of the algorithm to the original data points is shown in Fig. 17. The values of the parameters are shown in the insert box, as is the wavelength (in Angstroms). Simple reasoning from the algorithm shows that A_1 is the value of P in the direction of the sun ($\theta = 0$), and is thus closely related to the amount of multiple scattering which occurs. (For primary scattering $A_1 = 0$). The θ -dependent part of the second term is the Rayleigh phase function, so the magnitude of A_2 is closely related to the extent to which the system is dominated by Rayleigh scattering. Parameters A_3 and A_4 represent deviations from the Rayleigh curve, and are thus related to non-Rayleigh effects introduced by aerosol scattering in the atmosphere. Thus ideally the parameters should give a consistent interpretation of the physical state of the atmosphere as a scattering medium.

Anything like a complete discussion of the extent to which the ideal is achieved in the present study is beyond the scope of a short report. However, the general behavior of the parameters is shown in the following diagrams. Fig. 18 is a plot of A_1 versus wavelength for all of the data taken on March 25 at Mauna Loa. There is a clear trend in the data for the forenoon (dashed curves), in the sense of a generally decreasing negative magnitude of A_1 with increasing wavelength up to about $\lambda = 0.8\mu\text{m}$, beyond which A_1 becomes positive. This trend is a result of decreasing multiple scattering with increasing wavelength, and the disappearance of the neutral points mentioned above is a manifestation of the fact that $A_1 \geq 0$ at the longer wavelengths.

The behavior of A_1 during the afternoon of March 25, as shown by the solid curves of Fig. 18, is much less regular than that of the forenoon, due, in all probability, to the optical instability of the atmosphere which developed as the day progressed. A_1 became very small or positive throughout the range $0.6 \leq \lambda \leq 0.9\mu\text{m}$ except for an apparently anomalous period near sunset. There was little wavelength dependence of A_1 during the disturbed period, a fact which would indicate the predominance of aerosol effects over Rayleigh scattering at that time.

The dependence of A_1 on sun elevation at $\lambda = 0.32\mu\text{m}$ is shown for all of the measurements taken at Mauna Loa is shown by Fig. 19. The strong clustering

25 MAR 73 9:10 AM
 RUN 5 3200 A
 A1 = -0.043 +OR- 0.002
 A2 = 0.607 +OR- 0.002
 A3 = -0.002 +OR- 0.001
 A4 = 0.003 +OR- 0.001

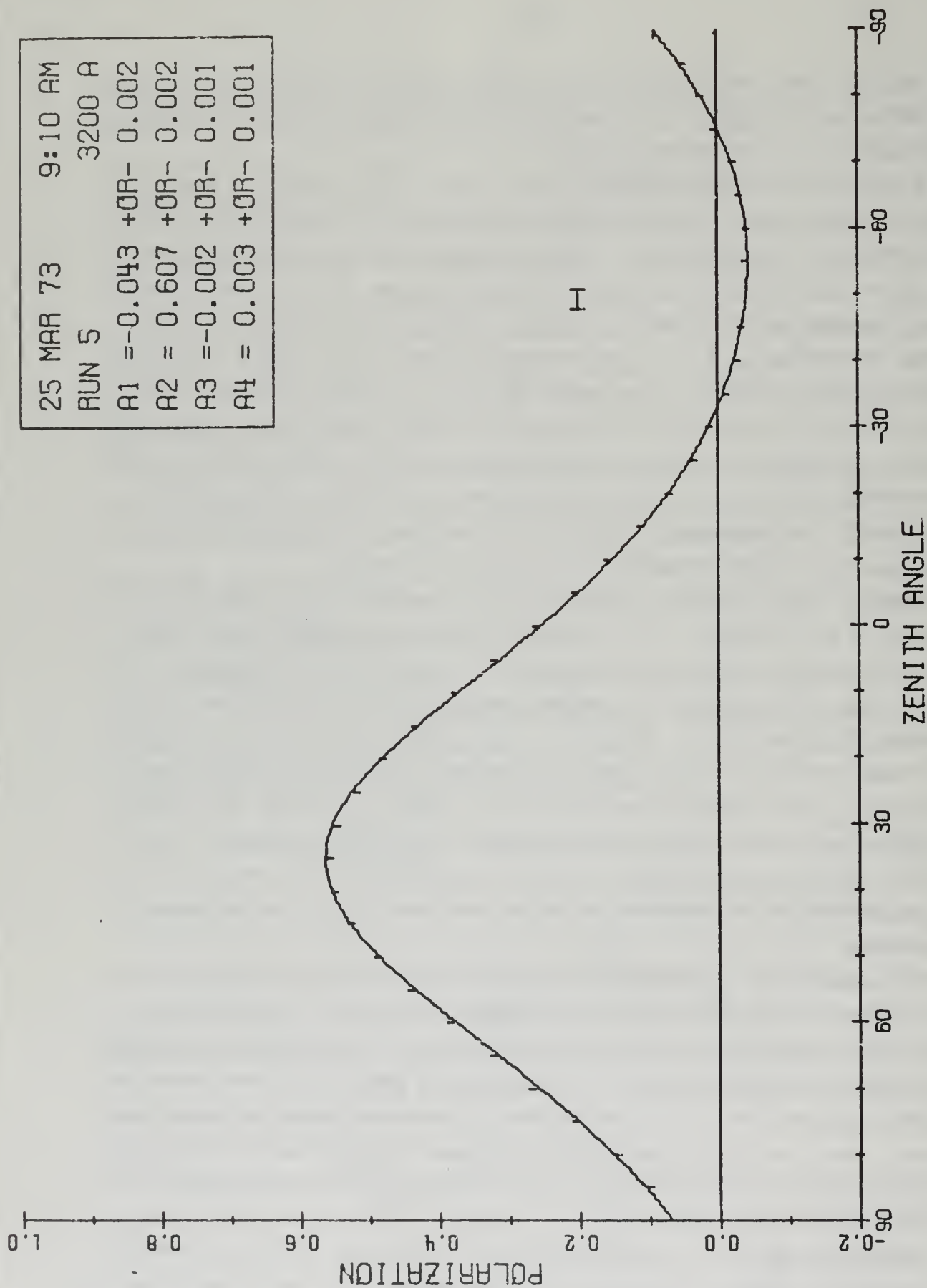


Fig. 17 Degree of polarization of skylight as observed at $\lambda = 0.32\mu\text{m}$ on Mauna Loa (plotted points) and as given by the parameterization algorithm Eq. (6) (solid line). Values of the derived parameters, together with

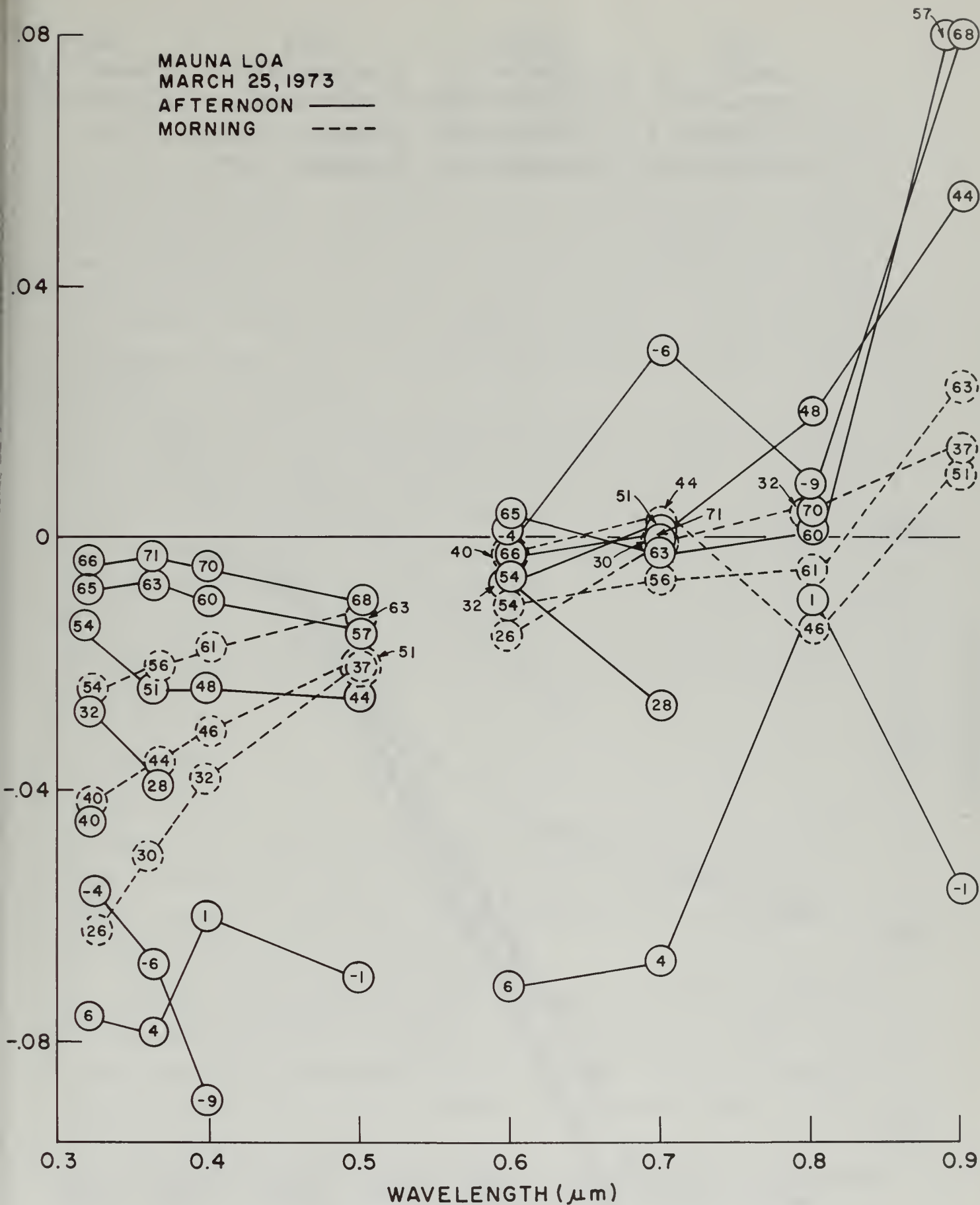


Fig. 18 Values of parameter A_1 as a function of wavelength for various scans of the sky at Mauna Loa on March 25, 1973. (--- forenoon; ——— afternoon).

1973		1973		1973		1973	
▽	JANUARY 31	⊙	FEBRUARY 7	◇	FEBRUARY 21	□	MARCH 24
◆	FEBRUARY 1	●	FEBRUARY 8	x	FEBRUARY 27	■	MARCH 25
○	FEBRUARY 2	◊	FEBRUARY 9	◊	MARCH 12		
△	FEBRUARY 6	△	FEBRUARY 20	◻	MARCH 22		

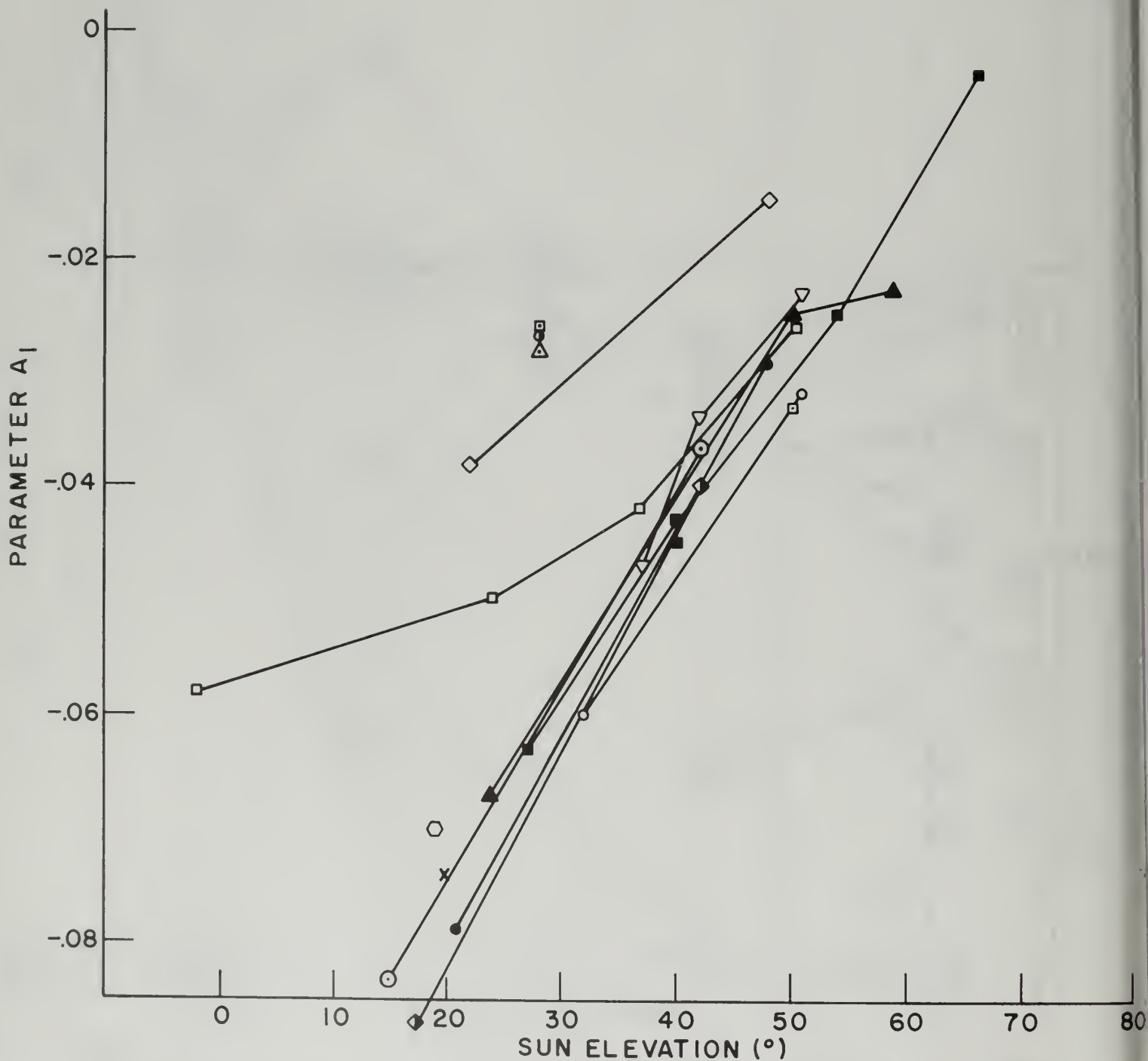


Fig. 19 Values of parameter A_1 at $\lambda = 0.32\mu\text{m}$ as a function of sun elevation for observations at Mauna Loa on the dates indicated.

of data points establishes well the general behavior of this parameter at the Mauna Loa observation site for a wavelength of $0.32\mu\text{m}$. On the basis of these data alone, it is not possible to say how sensitive A_1 at $\lambda = 0.32\mu\text{m}$ is to atmospheric turbidity. For instance the optical instability which developed during the afternoon of March 25 is not detected in these data, but anomalous results appeared at certain other times during the observation period. On physical reasoning alone one would expect this parameter to be more sensitive to turbidity at somewhat longer wavelengths, as in that case the Rayleigh scattering component plays a decreased role with respect to that of aerosol particles in the atmosphere.

Considerably more scatter of A_1 as a function of sun elevation is seen for $\lambda = 0.50\mu\text{m}$ in Fig. 20. This would seem to indicate a greater sensitivity to atmospheric conditions for $0.50\mu\text{m}$ than for $0.32\mu\text{m}$, but even here the increase of turbidity which appeared on the basis of other data to have occurred on the afternoon of March 25 is not well represented by these results.

The parameter A_2 is a measure of the total magnitude of the polarization variation, and is thus closely related to, but not identical with, the polarization maximum P_{max} . Observations show that the position of P_{max} is very close to $\theta = 90^\circ$. At this angle the parameterization algorithm reduces to

$$P(90^\circ) = A_1 + A_2 \quad (7)$$

or approximately

$$A_2 = P_{\text{max}} - A_1 \quad (8)$$

Generally A_1 is a negative quantity, in which case $A_2 > P_{\text{max}}$, but for the longer wavelengths $A_2 < P_{\text{max}}$. However, $A_1 \ll A_2$, so the behavior of A_2 should be similar to that of P_{max} , and the physical state of the system should be indicated as well by A_2 as by P_{max} .

Values of A_2 for the March 25 measurements made at Mauna Loa are plotted as a function of wavelength in Fig. 21. A comparison of this diagram with that of Fig. 5 shows that the patterns of A_2 and P_{max} are very similar, although the absolute magnitudes of the two are slightly different. The main point to be made is that the same deductions on atmospheric properties would be made from Fig. 21 as from Fig. 5.

The traditional methods of analyzing the polarization field do not take into account the distortion of the curve derived from the Rayleigh phase

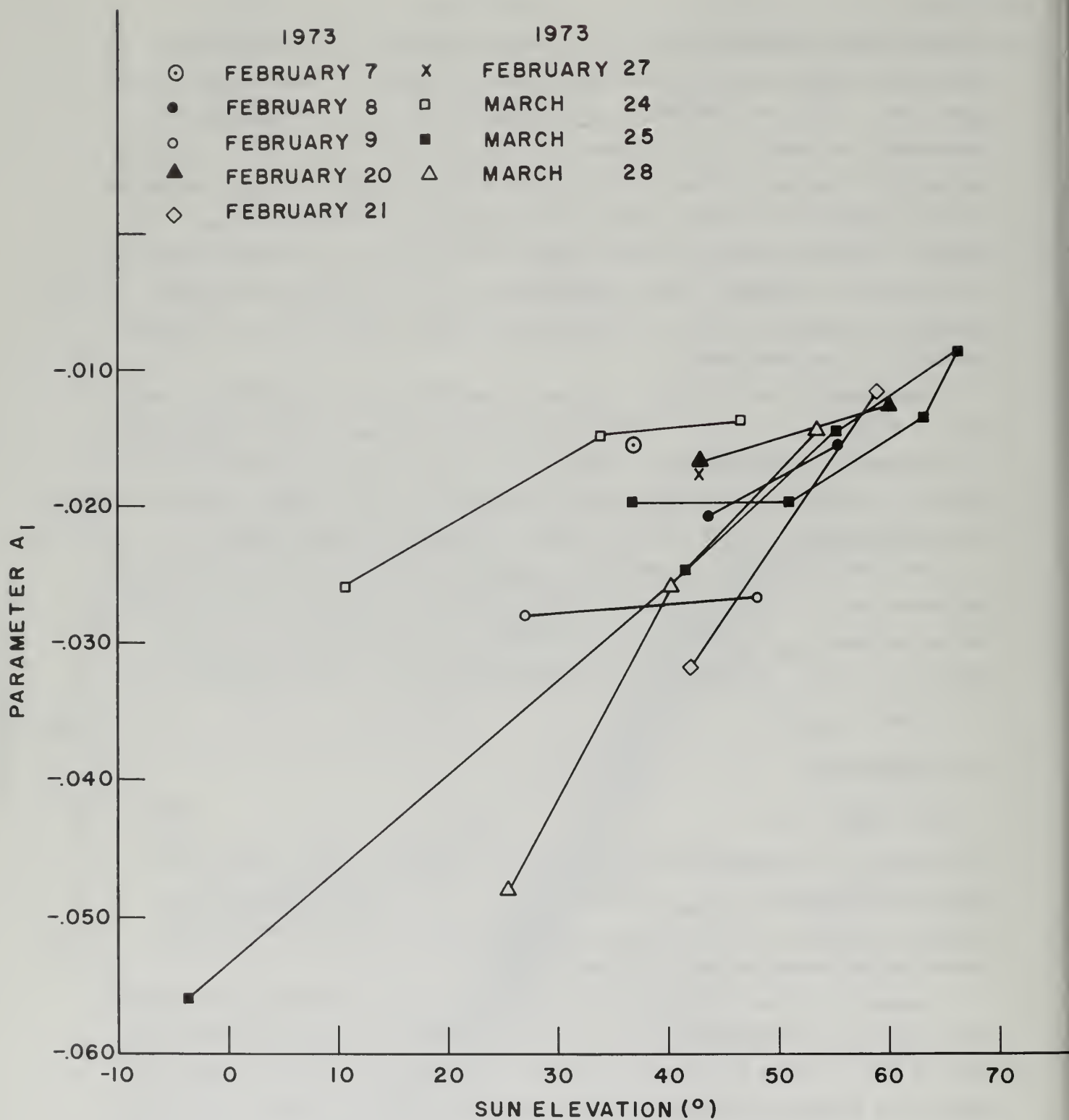


Fig. 20 Values of parameter A_1 at $\lambda = 0.50\mu\text{m}$ as a function of sun elevation for observations at Mauna Loa on the dates indicated.

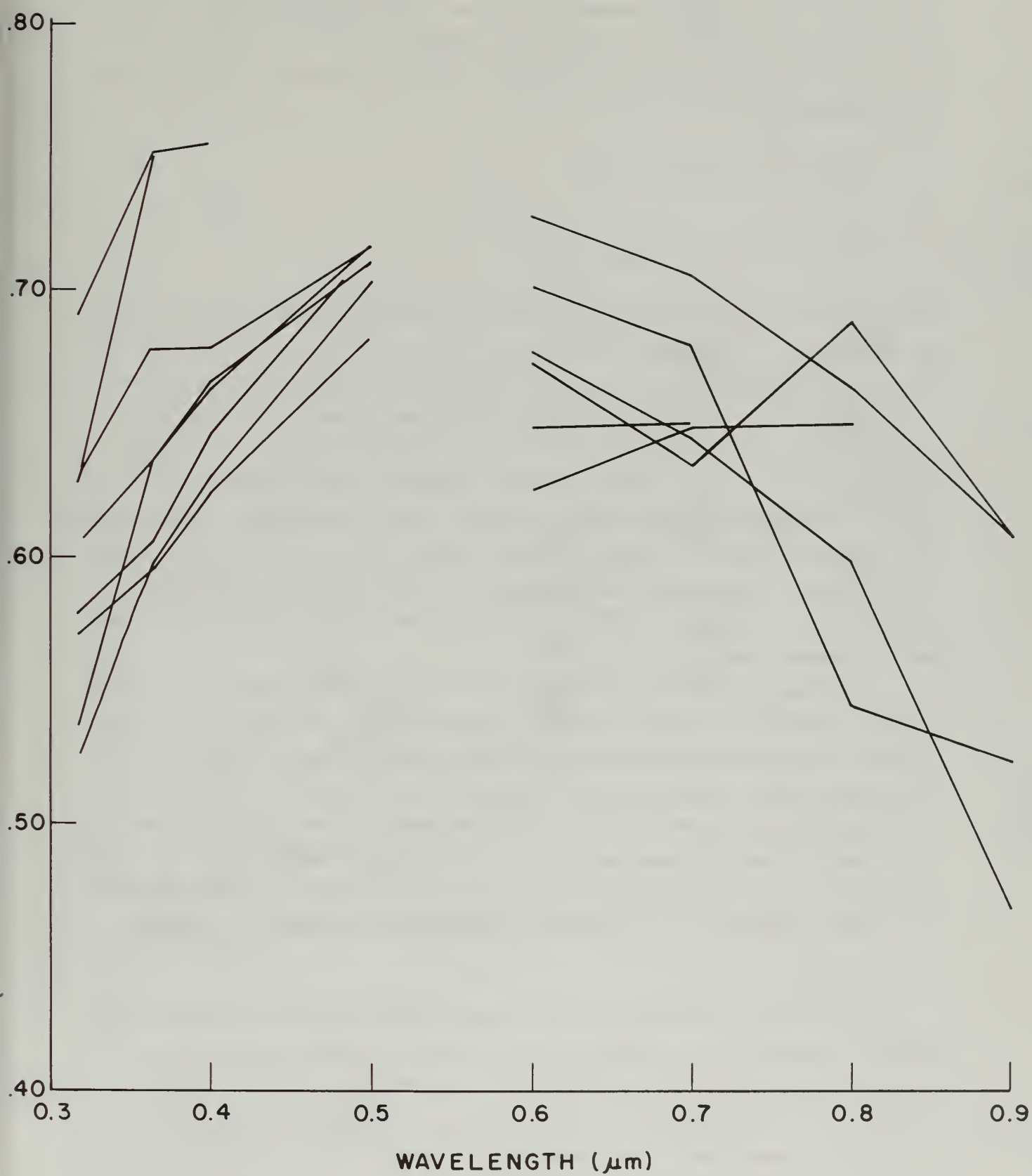


Fig. 21 Values of parameter A_2 as a function of wavelength for observations at Mauna Loa on March 25, 1973.

function due to aerosol effects. This is likely to be considerable, however, especially for the larger aerosol particles. The inclusion of the terms $A_3 \sin(2\theta)$ and $A_4 \sin(4\theta)$ in the parameter algorithm is an attempt to account for non-Rayleigh effects. For instance, at $\theta = 45^\circ$, $\sin 4\theta = 0$ and the algorithm reduces to

$$P(45^\circ) = A_1 + 0.33 A_2 + A_3 \quad (9)$$

or

$$A_3 = P(45^\circ) - A_1 - 0.33 A_2 \quad (10)$$

Since A_1 is small and the other terms are comparable in magnitude, A_3 would be expected to be relatively small, and to be sensitive to non-Rayleigh effects. By the same token, it would be sensitive to observational errors.

Values of A_3 as observed on March 25 on Mauna Loa, are plotted as a function of wavelength in Fig. 22. The fact that A_3 does tend to represent non-Rayleigh effects is indicated by the generally small magnitudes shown for short wavelengths and larger magnitudes for longer wavelengths. Unfortunately, the optical instability of the afternoon observations resulted in an increase of A_3 at short wavelengths and decrease at long wavelengths, which is contrary to what might be expected. The reason for this reversal is not clear at the present time.

The term $A_4 \sin(4\theta)$ has maxima at 22.5° and 67.5° , thereby indicating smaller deviations from the Rayleigh phase function. As with A_3 , the other terms of the parameterization algorithm are generally much larger than A_4 , and observational errors are very important in that case. In fact, A_4 in the Mauna Loa measurements appears to be dominated by random errors, and no clear pattern emerges from the data. It is likely, however, that for lower altitude stations where aerosol effects are more dominant, A_4 will prove to be a useful parameter as an empirical indicator of atmospheric turbidity.

VI Discussion

It had been anticipated that the polarization field of skylight above Mauna Loa would be very stable, and that the measurements would show a generally high degree of polarization with only minor variations. This thought was based on the facts that (1) the reflectance (albedo) of the lava in the vicinity of Mauna Loa is very low, and (2) that the atmosphere above the top

of the mountain is well above the trade wind inversion and thus protected from large amounts and variations of the aerosol content of the atmosphere. Thus any changes of aerosol content would be evidenced by small but distinct changes of the polarization field of skylight.

The data show that this expectation of a simple physical system was not borne out in reality. Large variations of the polarization field occurred over short periods of time, and while aerosol changes are evident in the data, there are definite indications of significant influences other than simple atmospheric scattering and reflection from the surrounding lava. A qualitative idea of these additional effects can be obtained from Fig. 23. The radiation entering the aperture of the polarizing radiometer is the sum of intensities I_p and I_m due to primary and multiple scattering of the original solar beam, plus the surface-reflected radiation which is scattered into the downward direction by the overlying atmosphere. Of these reflected components, I_1 due to reflection from the dark lava is very small because of the low reflectance of lava, and although it may be quite highly polarized, I_1 should not have much effect on the polarization of the total radiation stream.

Such is not the case, however, for components I_c and I_s due to reflection from clouds and from the sea surface. The albedo of clouds, particularly cumulus clouds, may be as high as 80% or more, so in the case of significant cloudiness surrounding the observation site, component I_c might well contribute a very significant part of the total observed intensity. Since I_c has generally low polarization, its main influence would be to decrease the magnitude of both the positive and negative branches of the polarization curve without changing appreciably the positions of the neutral points.

Table 2 gives a summary of all of the available information on cloudiness conditions existing on the days on which measurements were taken. The major part of the weather observations are those taken regularly by the National Weather Service at the Hilo airport. Since Hilo is on the windward side of the island, it is probable that the data represent the maximum of the cloudiness surrounding the island, and that the cloudiness on the western side of the island is generally less than that indicated by the weather observations. Satellite photographs of the area, taken at about noon each day by the ESSA-2 meteorological satellite, show the large scale features of the weather systems prevailing in the area. However, some of the cloud patterns were of a size below the resolution of the satellite

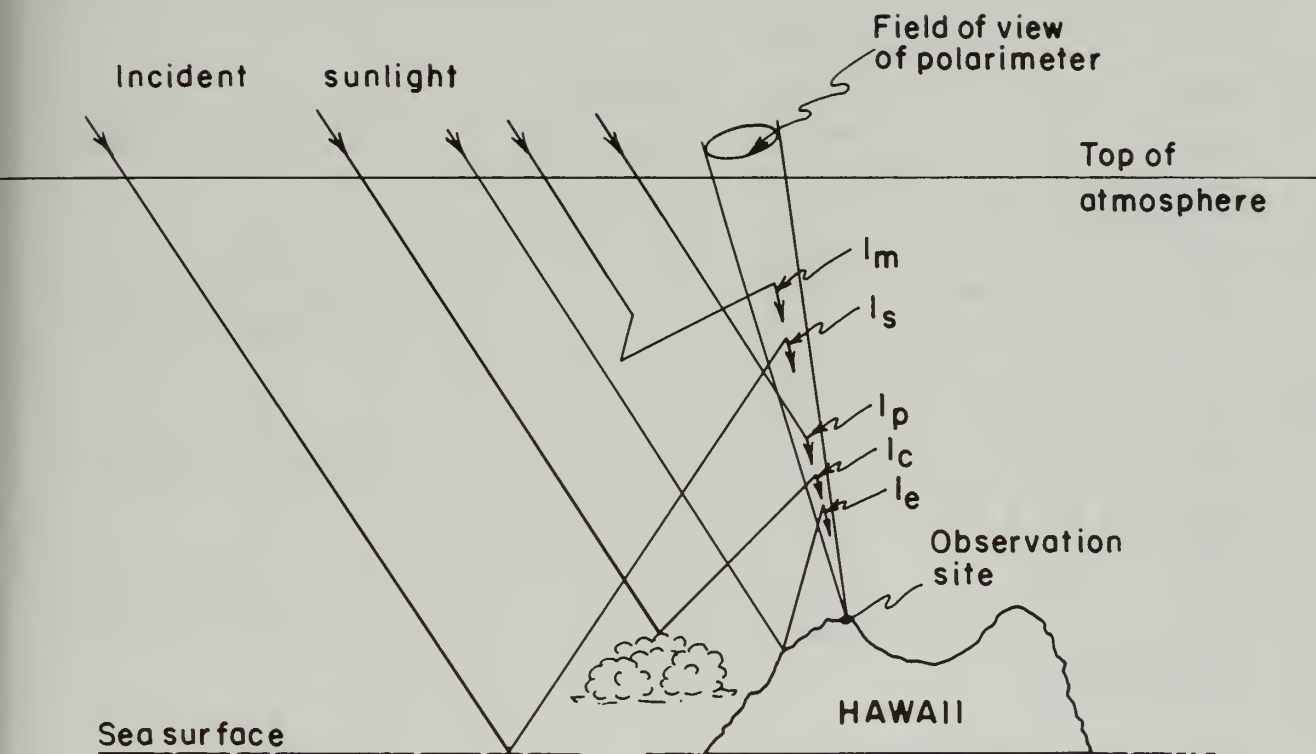


Fig. 23 Schematic diagram showing the main components of skylight incident at the Mauna Loa Observatory. (I_p : intensity due to primary scattering of direct sunlight by the atmosphere; I_m : intensity due to multiple scattering by the atmosphere; I_c : intensity due to reflection by clouds; I_s : intensity due to reflection by the sea surface).

Table 2. Types of clouds and total sky cover from the Hilo weather observation station and the large scale cloud indications from satellite photographs of the Pacific area.

Date (1973)	Local Std. Time	Clouds & Sky Cover (tenths)		Remarks	Indications from Satellite Photographs
		Cloud Types	Total		
1/31	0800	4 cu, 3 sc	6	Showers to E	
	1100	4 cu, 5 sc	8	" NE & along mts.	Cloudy N,E,S;clear W
	1400	3 cu, 1 sc	4		
2/1	0800	4 cu	4	Showers S	
	1100	1 cu	1	" W	Clear to scattered
	1400	1 cu, 8 sc	8	" SE	
2/2	0800	3 cu, 2 sc	5		
	1100	4 cu, 6 sc	8		Broken E,scattered W, front approaching
	1400	3 cu	3		
2/6	0800	3 cu, 8 sc	9		
	1100	2 cu, 6 sc	7		Clear all directions
	1400	1 cu, 1 sc	2		
2/7	0800	7 cu	7		
	1100	1 cu	1		Broken E,scattered W
	1400	1 cu	1		
2/8	0800	3 cu, 1 sc	4		
	1100	3 cu, 1 sc	4		Scattered
	1400	5 cu	5		
2/9	0800	4 cu, 1 sc, 3 ci	7		
	1100	5 cu, 1 sc	6		Scattered to broken
	1400	4 cu, 5 sc, 2 ci	9		
2/14	0800	3 cu, 6 sc	7		
	1100	4 cu, 5 sc	7		Broken E,scattered W
	1400	4 cu, 7 sc	9		
2/20	0800		0	Few cu, sc	
	1100		0	Few cu	Scattered
	1400	1 cu, 1 sc	2		
2/21	0800	7 cu, 3 sc	10	Light shower	
	1100	6 cu, 4 sc	9	Showers NE	Broken to overcast

Table 2 (cont.)

Date (1973)	Local Std. Time	Clouds & Sky Cover (tenths)		Remarks	Indications from Satellite Photographs
		Cloud Types	Total		
2/26	1400	6 cu, 5 sc	10	Showers NE	Overcast E, scattered W
	0800	2 fc, 10 cu	10	Light shower	
	1100	1 fc, 10 cu	10	Shower	
2/27	1400	1 fc, 5 cu, 4 sc	9	Showers S & along mts.	Broken E, scattered W
	0800	6 cu, 6 sc	10	Showers N & along mts.	
	1100	1 fc, 6 cu, 10 sc	10	Light shower	
	1400	4 cu, 7 sc	8	Showers along mts.	
3/2	0800	2 cu	2		Clear
	1100	2 cu, 1 ci	3		
	1400	3 cu, 6 sc	7		
3/5	0800	4 cu	4		Scattered to broken
	1100	3 cu	3		
	1400	4 cu	4		
3/22	0800	3 cu, 5 sc	6	Showers NE to SE	Scattered
	1100	2 cu	2		
	1400	3 cu	3		
3/23	0800	7 cu, 3 sc	9	Shower	Scattered
	1100	6 cu, 4 sc	9		
	1400	6 cu, 2 sc	7		
3/24	0800	6 cu, 3 sc	7	Light shower	Broken E, scattered W
	1100	6 cu, 6 sc	9		
	1400	7 cu, 3 sc	9		
3/25	0800	7 cu, 4 sc	10		Scattered to broken
	1100	7 cu	7		
	1400	3 cu	3		
	1700	4 cu, 1 sc	5		
	2000	4 cu	4		

Table 2 (cont.)

Date (1973)	Local Std. Time	Clouds & Sky Cover (tenths)		Remarks	Indications from Satellite Photographs
		Cloud Types	Total		
3/26	0800	1 cu, s sc, 6 ci	7		
	1100	2 cu, 9 cs	10		Broken to overcast cirrus
	1400	6 cu, 6 cs	10		
3/28	0800	6 cu, 4 sc	8		
	1100	3 cu, 3 sc	6		Scattered to broken
	1400	3 cu, 2 sc	4		

camera but still large enough to cause cloudiness on at least the east side of the island. This can be seen by the discrepancies in Table 2 between the Hilo cloud observations and the indications obtained from the satellite photographs. The photographs are sufficient to detect in many cases a strong asymmetry of the cloud pattern around the island, there being generally more extensive cloudiness on the windward side than on the lee side of the island. The effect of this asymmetry on the polarization measurements is difficult to assess.

Since the amount and distribution of cloudiness varied considerably during the period of observations, it is likely that some of the observed changes of the polarization field can be ascribed to relative changes of the cloud-reflected component I_c of the total skylight intensity.

Intensity component I_s due to reflection from the sea surface can be expected to have large variations of both magnitude and degree of polarization. For instance, the reflectance of a water surface is very high for large zenith angles of the sun, but it decreases in a nonlinear fashion to a low value of only 4 or 5% for the sun at the zenith. Likewise, for a still water surface, the degree of polarization of the reflected light varies from completely unpolarized at an angle of incidence of 0° to completely polarized at an angle of incidence equal to Brewster's angle (roughly 55 to 60°). It is likely that the wave structure of the actual sea surface would modify this pattern, but there is little doubt that component I_s was relatively strong and relatively highly polarized at times during the observation period. But there were probably times also, particularly during periods of large solar zenith angles, at which I_s was strong in relative magnitude but low in polarization, as well as times when I_s was effectively eliminated due to complete shading of the sea surface by extensive cloud cover. Thus the effects of I_s on the polarization of skylight at Mauna Loa are very difficult to evaluate without further information. They are, however, undoubtedly, responsible for at least a part of the changes which occurred during the observation period.

One possible indication of the effects of sea surface reflection on skylight polarization is the disappearance of the neutral points at wavelengths of 0.80 and $0.90\mu\text{m}$, and the existence of significant positive polarization in the vicinity of the sun at $\lambda = 0.90\mu\text{m}$. On the basis of this hypothesis,

the polarization field at shorter wavelengths would be dominated much less by sea surface reflection, because of the increase of optical thickness of the atmosphere with decreasing wavelength. The incoming beam would be scattered much more strongly during its initial traverse of the atmosphere at short than at long wavelengths, thereby making the sum $I_p + I_m$ due to atmospheric scattering strong at short wavelengths and weak at long wavelengths. For the same reason, shortwave radiation reaching the ocean surface and reflected into the field of view would be strongly attenuated in both its inward and outward traverses. At long wavelengths, on the other hand, $I_p + I_m$ is small, and the small amount of attenuation of the solar beam during both its inward and outward traverses of the atmosphere would tend to make I_s a significant part of the total observed radiation. Thus the polarization field should be particularly sensitive to sea surface reflection at the longer wavelengths.

To indicate this effect of wavelength somewhat more quantitatively, we compare the Rayleigh optical thicknesses of the atmospheric path of component I_s at $\lambda = 0.32$ and $\lambda = 0.90$ for zenith angles of the sun at 30° and 60° in Table 3. The Rayleigh assumption, of course, does not admit aerosol effects, but the atmosphere in the region of Hawaii is not heavily aerosol laden. Furthermore, the additional optical thickness due to aerosols would tend to increase the effect under discussion.

Table 3. Approximate optical pathlength τ and fractional transmission T at wavelengths of 0.32 and 0.90 μ m for the intensity component I_s due to sea surface reflection for locations at the sea surface itself, at the observation site, and at the top of the atmosphere for two different zenith angles θ_o of the sun.

Location/Wavelength	$\theta_o = 30^\circ$				$\theta_o = 60^\circ$			
	0.32 μ m		0.90 μ m		0.32 μ m		0.90 μ m	
	τ	T	τ	T	τ	T	τ	T
At sea surface	0.805	0.447	0.015	0.985	1.40	0.247	0.026	0.974
At observation site	0.986	0.373	0.019	0.981	1.76	0.172	0.033	0.967
At top of atmosphere	1.61	0.200	0.030	0.970	2.80	0.061	0.052	0.949

Table 3 shows that the optical pathlengths for radiation of $\lambda = 0.90\mu$ m are quite small, thereby permitting a transmission of 95% or better for component I_s for all cases tabulated. Conversely, the large optical pathlength

for $\lambda = 0.32\mu\text{m}$ yields transmission values from about 45% to only 6%, depending on conditions. For this reason, the influence of sea surface reflection on the polarization field at Mauna Loa would be much greater at $\lambda = 0.90\mu\text{m}$ than at $\lambda = 0.32\mu\text{m}$, in accord with the measurements.

VII Conclusions

The measurements of skylight polarization made at an altitude of approximately 11,200 feet on Mauna Loa, Hawaii, during the period January to March 1973 support the following conclusions:

1. The polarization field of skylight at Mauna Loa is much more variable than had been anticipated. The variability appears to be produced by changes of the reflection properties of the sea surface and clouds surrounding the Observatory, as well as by changes of the aerosol content of the atmosphere above the level of the Observatory.
2. This short series of observations was insufficient to adequately assess the potential of skylight polarization measurements as an indicator of atmospheric aerosols at Mauna Loa. Although some reasonably definite aerosol effects were observed, they were intermixed with surface reflection variations, and difficult to isolate completely. For this reason, future measurements for aerosol characterization alone should be concentrated in periods of uniform cloud conditions, the ideal situation being cloudless conditions both above and below the level of the Observatory. Appropriate cases of this ideal could be selected from any long series of observations, in which case the skylight polarization will be a useful parameter for monitoring the environment.
3. Future investigations of skylight polarization on Mauna Loa should include measurements of the Stokes parameters, including total intensity, in the region near the disk of the sun. The present and previous data show that both polarization and intensity in the aureole region are sensitive to aerosol conditions, particularly at the longer wavelength. This is further confirmed by the observations of Dr. Hansen and his colleagues on Mauna Loa. Measurements of the intensity gradients in the aureole will provide data for a deduction of the size-frequency distribution of the scattering particles.
4. Because of the strong effects of surface reflection evident in the present measurements, it is probable that the polarization method will be simpler

to apply for the case of uniform surface albedo over a large region surrounding the observation site. Such uniform surfaces occur in desert regions, in heavily forested areas, and in regions of extensive snow cover. Of particular interest in the last of these is the program of intensity and polarization measurements of skylight being planned to start in December 1974 at the geographical South Pole.

5. A scheme has been developed for parameterizing polarization measurements for greater facility in handling the data and convenience in their analysis and interpretation.
6. The computer-controlled polarizing radiometer which was recently developed for studies of skylight polarization performed well, for both automatic acquisition of the measurements and real-time reduction of the data, during the period. It demonstrated in a convincing fashion that photon counting techniques are entirely applicable for the skylight measurements, and that very high precision may be achieved in a reasonable integration time by the method.

VIII References

- Coulson, K. L. (1952) "Polarization of Light in the Sun's Vertical," Sci. Rept. No. 4, Contr. AF 19(122)-239, Univ. of California, Los Angeles.
- Coulson, K. L. (1971) "On the Solar Radiation Field in a Polluted Atmosphere," J. Quant. Spectrosc. Radiat. Transfer, 11, 739-755.
- Coulson, K. L., J. V. Dave, and Z. Sekera (1960) Tables Related to Radiation Emerging from a Planetary Atmosphere with Rayleigh Scattering, Univ. of California Press.
- Coulson, K. L., and R. L. Walraven (1972) "A High-Precision Computer-Controlled Dual-Channel Polarizing Radiometer," Conference on Atm. Rad., Am. Met. Soc., Fort Collins, Colo., Aug. 7-9, 1972.
- Dorno, C. (1919) "Himmelshelligkeit, Himmelpolarisation, und Sonnenintensitat in Davos (1911 bis 1918)," Met. Zeit., 36, 109-124, 181-192.
- Neuberger, H. (1950) "Arago's Neutral Point: A Neglected Tool in Meteorological Research," Bul. Am. Met. Soc., 31, 119-125.
- Pyaskovskaya-Fesenkova, E. V. (1958) "On Scattering and Polarization of Light in Desert Conditions," Doklady Akad. Nauk, USSR, 123:6, 1006-1009 (in Russian).

Pyaskovskaya-Fesenkova, E. V. (1960) "Some Data on the Polarization of Atmospheric Light," Doklady, Akad. Nauk, USSR 131:2, 297-299 (in Russian).

Sekera, Z. (1957) "Polarization of Skylight," Encyclopedia of Physics, Springer Pub. Co., 48, 288-328.

Soret, J. L. (1888) "Influence des Surfaces d'Eau sur la Polarisation Atmosphérique et Observation de deux Points Neutres a droite et a gauche due Soleil," C. R. Acad. Sci., Paris, 107, 867-870.

Stamov, D. G. (1970) "The Necessity of Accurate Quasi-Empirical Relations for Summarizing Observations of Skylight Polarization," Collected Works, Atmospheric Optics, 138-144 (in Russian).

IX Acknowledgements

It is a pleasure to acknowledge with thanks the contributions of several persons in this series of measurements and data interpretation. The hospitality and cooperation of Dr. Ronald Fegley and his colleagues at the Mauna Loa Observatory was not only valuable for the observational work, but it made the task a pleasant one as well. Observatory personnel exceeded all reasonable expectations by even taking some of the polarization measurements during the absence of the regular operators. The Meteorologist in Charge of the Hilo weather station, in cooperation with Dr. Fegley, supplied copies of the Hilo observations for the period, and Mr. Alvin J. Miller of the Air Resources Laboratories, Silver Spring, Maryland, was kind enough to obtain satellite photographs of the Pacific area for the days of the observations. Mr. Douglas Hoyt, Air Resources Laboratories, Boulder, Colorado, made a special effort to speed up the normal processing of the radiation measurements of the Mauna Loa Observatory, for which we are grateful. Special thanks go also to Martin Miller, Robert Hamilton, and Bruce Fitch, students in Atmospheric Science, for their careful processing and plotting of the data.

**RETURN TO the circulation desk of any
University of California Library**

or to the

NORTHERN REGIONAL LIBRARY FACILITY

University of California

Richmond Field Station, Bldg. 400

1301 South 46th Street, Richmond, CA 94804-4698

ALL BOOKS MAY BE RECALLED AFTER 7 DAYS

To renew or recharge your library materials, you may
contact NRLF 4 days prior to due date at (510) 642-6233

DUE AS STAMPED BELOW

OCT 26 2011

DD20 10M 4-10

